Journal of Dermatological Science 62 (2011) 50–57

Contents lists available at ScienceDirect

Journal of Dermatological Science

journal homepage: www.elsevier.com/jds

Enhancement of nickel elution by lipopolysaccharide-induced inflammation

Rina Tanaka [a], Yoshiaki Goi [a], Kenji Ishihara [b], Kyosuke Ueda [c], Takayuki Narushima [c], Hiroshi Ohtsu [c], Masahiro Hiratsuka [a], Noriyasu Hirasawa [a,*]

[a] Graduate School of Pharmaceutical Sciences, Tohoku University, Japan
[b] Course for School Nurse Teacher, Faculty of Education, Ibaraki University, Japan
[c] Graduate School of Engineering, Tohoku University, Japan

ARTICLE INFO

Article history:
Received 20 August 2010
Received in revised form 25 December 2010
Accepted 27 December 2010

Keywords:
Nickel release
Lipopolysaccharide
In vivo model
In vitro model
RAW 264 cells

ABSTRACT

Background: Implantations of metallic biomedical devices into bodies are increasing. The elution of Ni ions from these devices can lead to metal allergies. However, the molecular mechanisms of the elution have not been fully examined. Furthermore, it is not clear whether infection and inflammation affect the corrosion of metals.
Objective: We examined whether the elution of Ni from metal wires and plates was enhanced by inflammation *in vivo* and *in vitro*.
Methods: A Ni or SUS316L wire was implanted subcutaneously in the dorsum of mice. Lipopolysaccharide (LPS) was injected at the site immediately following the implantation. After 8, 24, and 72 h, the tissue around the wire was excised. RAW 264 cells were seeded on a Ni plate and incubated for 24 h in medium containing LPS. The amount of Ni in the tissue or conditioned medium was determined fluorometrically.
Results: The release of Ni ions from the wire was significantly increased from 8 to 72 h, and further increased by LPS. LPS also enhanced the release of Ni ions by the cells, but only when they were attached to the Ni plate. Chloroquine, bafilomycin A_1 and amiloride markedly inhibited the effects of LPS.
Conclusion: The activation of inflammatory cells on metals enhanced the elution of Ni probably via the release of protons at the interface of the cells and material.

1. Introduction

Implantations of biomedical devices to treat diseases and organ insufficiencies are increasing as populations age [1]. Most devices for the replacement of hard tissues, including artificial hip joints, bone plates and dental implants, comprise metallic biomaterials because of their reliable mechanical performance [2,3]. Corrosion-resistant and ductile, nickel (Ni) is contained in various alloys, including stainless steels, Ni–Cr and Ni–Ti. However, Ni is also the most common contact allergen among metals [4]. Allergies to Ni, classified as Type IV allergies [5], are initiated by the release of Ni ions from alloys. Ni bound to soluble proteins [4] or to proteins on antigen-presenting cells [6] is recognized as an antigen. The antigen-presenting cells then activate T cells and induce an increase in the number of Ni-specific, IFN-γ-producing $CD4^+$ and $CD8^+$ effector T cells [7]. It is difficult to prevent Ni allergies by inhibiting these immune responses. A more practical approach might be to block the elution of Ni ions from biomaterials. However, the molecular mechanisms of this elution have not been fully examined. Furthermore, although the inflamed sites become acidic, it is not clear whether infection and inflammation affect the corrosion of metals.

In general, the release of Ni ions from alloys is tested in solutions [8,9]. However, as biodevices are implanted for long periods of time, one should test the release of metal ions from alloys in tissues to assess the risk of inducing metal allergies. There is little evidence that the release of metal ions from alloys *in vivo* is similar to that *in vitro*.

To reveal the mechanisms of Ni-induced inflammation and allergy, several animal models have been developed. The injection of Ni ions into sensitized animals was found to cause allergic inflammation including ear swelling [8–10], footpad edema [11] and the proliferation of lymph node cells [12]. Tolerance to nickel sensitization was also examined in these animals [9]. Recently, Sato et al. found that the co-administration of lipopolysaccharide (LPS), a stimulator of innate immune responses [13], effectively enhanced sensitization to Ni [10]. Sensitization using Ni ions plus LPS will promote research into how metal allergies are evoked. In contrast to models using Ni ions, we induced inflammation in mice using a Ni

* Corresponding author at: Laboratory of Pharmacotherapy of Life-style Related Diseases, Graduate School of Pharmaceutical Sciences, Tohoku University, 6-3 Aoba Aramaki, Aoba-ku, Sendai, Miyagi 980-8578, Japan. Tel.: +81 22 795 5915; fax: +81 22 795 5504.
E-mail address: hirasawa@mail.pharm.tohoku.ac.jp (N. Hirasawa).

0923-1811/$36.00
doi:10.1016/j.jdermsci.2010.12.006

wire [14]. In this model, Ni wire but not Fe, Al and Co wires induced necrosis of the surrounding tissues. The implantation of the Ni wire elicited the increase in plasma exudation 8 h after the implantation and prostaglandin and histamine mediated the responses, indicating that Ni ions were released within a few hours [14].

LPS mimics the inflammation induced by an infection, which can occur when a biomedical device is implanted [15,16]. Therefore, it is possible that the injection of LPS enhances the elution of Ni ions from metals. In this study, using Ni wire-induced inflammation model and a novel *in vitro* system, we examined the mechanisms responsible for the elution of Ni.

2. Materials and methods

2.1. Animals

Male C57BL/6 mice, specific pathogen free and weighing 22–25 g, were purchased from SLC (Shizuoka, Japan). The mice were treated in accordance with procedures approved by the Animal Ethics Committee of Tohoku University, Japan.

2.2. Materials

A Ni wire (>99%, ϕ 0.8 mm), a SUS316L wire (ϕ 1 mm), and a Ni plate (>99%, thickness: 0.05 mm) were purchased from Nilako Co., Tokyo, Japan. Lipopolysaccharide (LPS) was purchased from Sigma–Aldrich (St. Louis, MO) and amiloride, chloroquine, and bafilomycin A_1 were from Wako Pure Chemical Ind. (Osaka, Japan).

2.3. Implantation of the Ni wire into mice

A nickel wire and a SUS316L wire were cut into 5 mm lengths and sterilized by soaking in ethanol. Mice were anesthetized and a length of wire was implanted subcutaneously in the dorsum using a 13G implant needle (Natsume Co., Tokyo, Japan). A hundred microliters of LPS solution (1 μg/ml) or saline was injected into the site immediately after the implantation. The mice were sacrificed at the indicated time and then the skin tissue (diameter: 14 mm) on the wire was excised. The skin samples were minced with scissors in 500 μl of Milli Q water and left at 4 °C overnight. The extract was centrifuged at 15,000 rpm for 20 min, and the supernatant was used to determine Ni concentrations as described below.

2.4. Determination of Ni concentrations by fluorometry and ICP-AES

Samples were diluted with Milli Q water, and Newport Green DCF [17] was added (150 μl per tube: 0.75 μM) to 850 μl of diluted sample. Fluorescence intensity was determined with excitation and emission wavelengths of 505 and 535 nm, respectively, with the use of a Fluorometer F-2000 (Hitachi High-Technologies Corporation, Japan). The Ni concentrations of some samples were determined by inductively coupled plasma atomic emission (ICP-AES) with an ICPS-8000 (Shimadzu System Development Corporation, Japan).

2.5. Macroscopic and histochemical analyses

Mice were sacrificed 0, 8, 24, or 72 h after the implantation. Tissue (14 mm in diameter) including epidermis, dermis and subcutaneous tissue on the wire was then excised and weighed. The wires obtained were washed with phosphate-buffered saline and then with an ice-cold lysis buffer (20 mM HEPES, pH 7.4, 1% (v/v) Triton-X 100, 10% (v/v) glycerol) to remove attached cells. The surface of wires was observed by scanning electric microscope (S-3200N, Hitachi, Japan).

2.6. Incubation of the Ni wire in vitro

A Ni wire was incubated in 50 μl of Milli Q water, saline, or mouse serum at 37 °C for 8 h. Then, the amount of Ni eluted was determined as described above.

2.7. Cell culture and stimulation

RAW 264 cells, mouse macrophage cell lines, were cultured at 37 °C under 5% CO_2–95% air in phenol red-free Eagle's minimal essential medium containing 10% (v/v) fetal bovine serum, penicillin G potassium (15 μg/ml), and streptomycin sulfate (50 μg/ml). The cells were suspended at the indicated numbers in the same medium, and 200 μl of the cell suspension was added to a Ni plate (25 mm^2) in each well of a 96-well cluster dish. Two hours later, LPS was added at the indicated concentrations and the cells were further incubated at 37 °C for 24 h or the period indicated. To prevent them attaching to plates, the cells were seeded first, and 2 h later, the Ni plate was placed in a sloping position into each well.

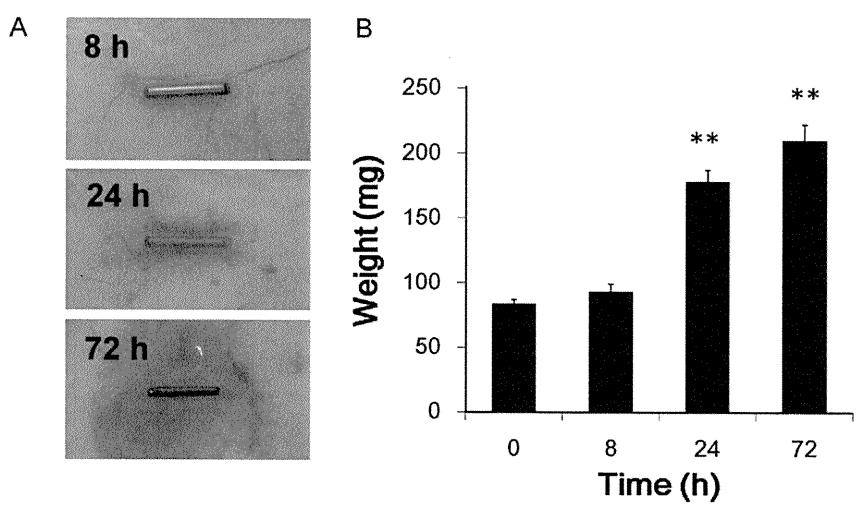

Fig. 1. Ni wire-induced inflammation. (A) A Ni wire was implanted subcutaneously in the dorsum of each mouse. The mice were sacrificed 8, 24 and 72 h after the implantation, and the skin around the wire was photographed. (B) The skin tissue (diameter: 14 mm) on the wire was excised and the weight of tissue was measured. The values are means for four mice with the S.E.M. shown by vertical bars. Statistical significance: $^{**}P < 0.01$ vs. the 0 h group.

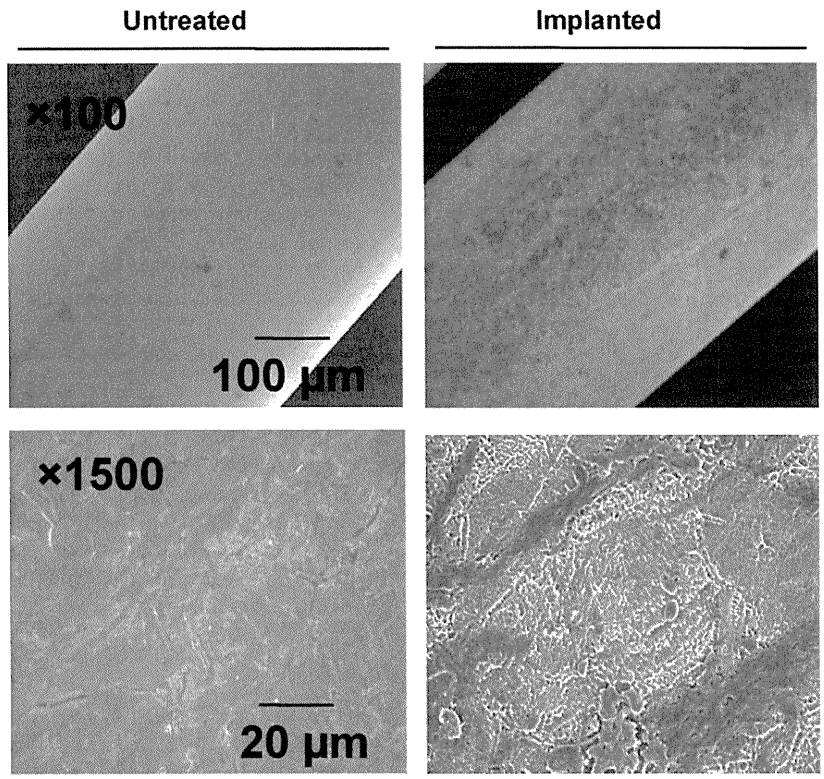

Fig. 2. Erosion of the surface of Ni wire. The surface of an untreated Ni wire (left) and an implanted Ni wire 72 h after implantation (right) was analyzed by scanning electron microscope.

2.8. Drug treatment

The V-ATPase inhibitor bafilomycin A_1 [18] was dissolved in DMSO, and the lysosome inhibitor chloroquine [19], and the Na^+/H^+ exchanger (NHE) inhibitor amiloride [20,21], were dissolved in autoclaved water, and diluted with the medium. The cells were incubated at 37 °C for 10 min in 1 ml of medium containing bafilomycin A_1 (1 nM), amiloride (100 μM), or chloroquine (10 μM) and then stimulated with LPS as described above. The final concentration of DMSO was 0.1% (v/v).

2.9. Statistical significance

The statistical significance of the results was analyzed with Dunnett's test or the Student–Newman–Keuls test for multiple comparisons. The results were confirmed by at least three independent sets of experiments.

3. Results

3.1. Metal wire-induced inflammation

A Ni wire was implanted subcutaneously into the dorsum of C57BL/6 mice and the response was observed 8, 24 and 72 h later. Consistent with our previous study, the wire caused extreme inflammation and bleeding (Fig. 1A). As an index of edema formation of tissues, the weight of skin tissues (14 mm in diameter) including epidermis, dermis and subcutaneous tissue on the wire was determined. The skin weight on the wire was

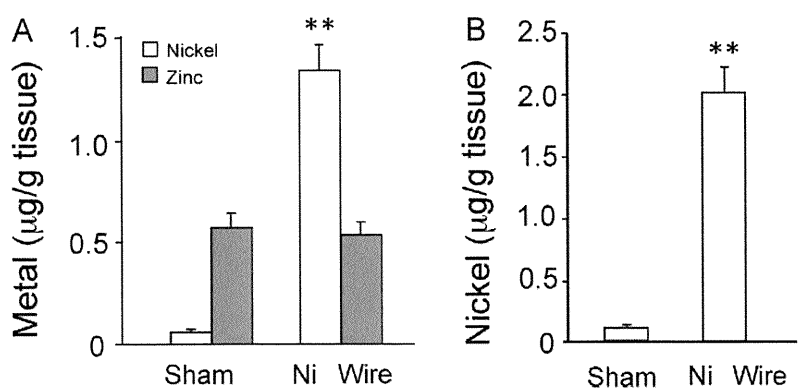

Fig. 3. Determination of the amount of Ni ions in tissues. (A) Skin tissue (diameter: 14 mm) was excised 8 h after the implantation of the Ni wire or sham treatment, and minced in 500 μl of deionized water. The concentrations of Ni and Zn ions in the supernatant were determined by ICP-AES. Values are the means for four mice with the S.E.M. shown by vertical bars. Statistical significance: $^{**}P < 0.01$ vs. the corresponding sham control group. (B) The concentrations of Ni in the same samples were determined by fluorometry. Values are means for four mice with the S.E.M. shown by vertical bars. Statistical significance: $^{**}P < 0.01$ vs. the sham group. The coefficient of the correlation between the concentrations of Ni ions determined by fluorometry (B) and by ICP-AES (A) was 0.996.

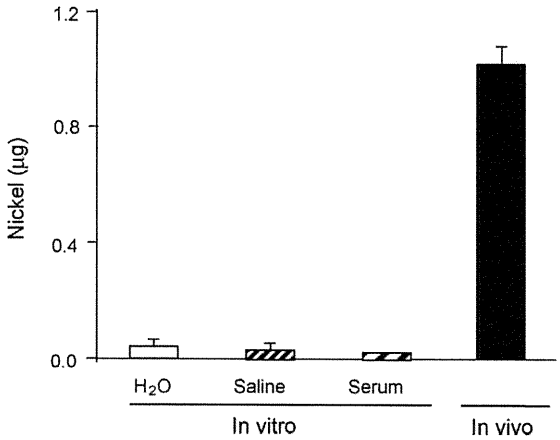

Fig. 4. Comparison of the release of Ni ions from a Ni wire *in vivo* and in solutions. A Ni wire was incubated at 37 °C for 8 h in 50 μl of H_2O, saline and serum. Then, Ni ions in the solution were quantified by fluorometry. The amount of Ni ions in the tissue 8 h after the implantation was determined as described in Fig. 3, and described as "*in vivo*". The values are the means of the four samples with S.E.M. shown by vertical bars.

significantly increased at 24 and 72 h (Fig. 1B), indicating that plasma leakage was induced by the Ni wire.

3.2. Corrosion of the wire

The corrosion of the implanted wire was analyzed with a scanning electron microscope. The untreated wire was smooth (Fig. 2, left panels) but the wire obtained 72 h after the implantation showed numerous traces of corrosion (Fig. 2, right panels), indicating that Ni ions had been released.

3.3. Quantitative analysis of the elution of Ni

A Ni wire was implanted subcutaneously in the dorsum and the skin tissue on the wire was excised 8 h later and homogenized. To evaluate quantitatively the release of Ni from the wire, the amounts of Ni ions, and Zn ions, as an internal control, in the supernatant of the skin tissue-homogenate were quantified by ICP-AES (Fig. 3A). The amount of Ni ions in the tissue was increased, although that of Zn ions was unchanged. Then we determined the concentration of Ni ions in the same sample by fluorometry using Newport Green DCF. As shown in Fig. 3B, the measurement of the Ni concentration in the control skin was not disturbed by Zn ions and the values showed a good correlation with those obtained by ICP-AES ($r = 0.996$). Therefore, in the experiment that followed, we determined the amount of Ni ions in the tissue by fluorometry.

3.4. Elusion of Ni ions in vivo and in solution

A Ni wire was incubated at 37 °C for 8 h in an aliquot of water, saline, or serum of C57BL/6 mice. The concentrations of Ni ions in the aliquots of water, saline and serum were only small as compared with the amount detected in the tissue homogenate (Fig. 4). These results suggested that Ni was eluted much more easily *in vivo* than *in vitro*.

3.5. Enhancement of the release of Ni from Ni- and SUS316L-wire in vivo by LPS

Using the wire-implanted mice, we found that the release of Ni ions was detectable at 8 h and increased to at least 72 h after the implantation. LPS (1 μg/100 μl saline) or saline (100 μl) was injected into the same site immediately after the implantation. Histological analysis disclosed that the wire's presence induced the infiltration of inflammatory cells, such as neutrophils and macrophages, in the tissue and LPS remarkably enhanced this process (Fig. 5A). The amount of Ni ions in the tissue samples from the LPS-treated group was significantly increased compared with that for the saline-treated group. The difference was significant at 8 and 24 h after the implantation (Fig. 5B).

Then we examined whether Ni was eluted from SUS316L, which is used as biomedical device. When SUS316L-wire was implanted subcutaneously in the dorsum of the mice, only a little elution of Ni ions was observed at 72 h after the implantation. As consistent with Ni wire, the elution of Ni from SUS316L wire was enhanced by the injection of LPS (Fig. 6).

3.6. Enhancement of the release of Ni ions from a metal plate by activated macrophages

Because macrophages are involved in the first line of defense in the inflammatory and immune response to foreign materials in

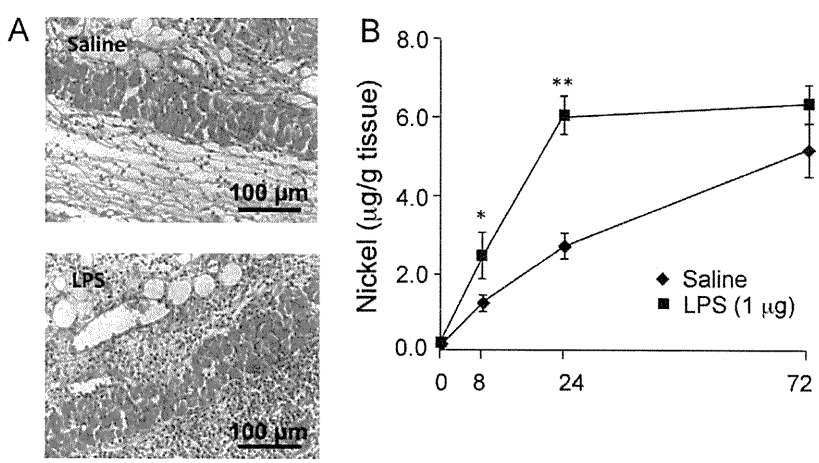

Fig. 5. Increase in the release of Ni ions by LPS-induced inflammation. (A) A Ni wire was implanted subcutaneously in the dorsum of each mouse. LPS (1 μg, bottom) or vehicle (saline, top) was injected into the site immediately after the implantation. Twenty-four hours after the implantation, the mice were sacrificed and the skin on the wire was dissected. Sections of tissue were prepared and stained with hematoxylin–eosin. (B) The skin tissue (diameter: 14 mm) on the wire was excised 8, 24 and 72 h after the implantation of Ni wires and the Ni ions in the tissue were quantified by fluorometry. Values are means for five mice with the S.E.M. shown by vertical bars. Statistical significance: $^{*}P < 0.05$, $^{**}P < 0.01$ vs. the saline group at the corresponding point.

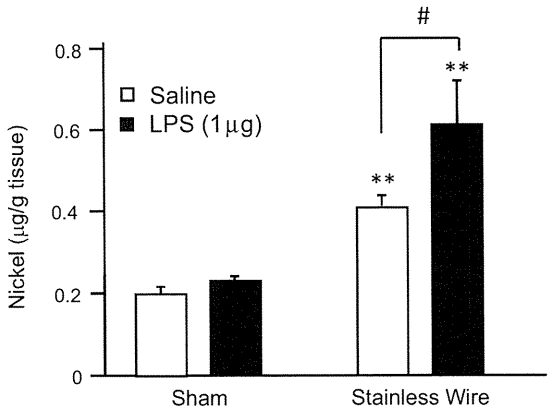

Fig. 6. Increase in the release of Ni ions from SUS316L by LPS. A SUS3167L-wire was implanted subcutaneously in the dorsum of each mouse. LPS (1 μg, closed columns) or vehicle (saline, open columns) was injected into the site immediately after the implantation. Seventy-two hours after the implantation, the mice were sacrificed and the skin tissue (diameter: 14 mm) on the wire was excised. The Ni ions in the tissue were quantified by fluorometry. Values are means for five mice with the S.E.M. shown by vertical bars. Statistical significance: $^{**}P < 0.01$ vs. the corresponding sham group, and $^{\#}P < 0.05$ between groups indicated.

many tissues, we examined whether these cells induced the release of Ni ions from metals by using a mouse macrophage cell line RAW 264. RAW 264 cells were seeded on a Ni plate (25 mm^2) and incubated for 24 h in the presence or absence of LPS (1 μg/ml). Although few Ni ions were released when the plate was incubated in medium alone, the amount increased in the presence of the cells (Fig. 7A). Interestingly, the stimulation of the cells with LPS significantly increased the release of Ni ions in a concentration- and time-dependent manner (Fig. 7B and C). These results suggested that the activated cells enhanced elution of Ni ions from the plate.

3.7. Change in pH of the conditioned medium

To clarify whether the elusion of Ni ions from plates was caused by acidification of the medium, the pH of the conditioned medium was determined. The pH of the conditioned medium collected after the 24-h incubation decreased dependent on the number of cells (Fig. 8A) but was not affected by the addition of LPS (Fig. 8B). These findings indicated that the acidification of the medium was induced by the respiratory metabolism of cells and was not the main cause to induce Ni elution.

3.8. Requirement of cell attachment to the metal

We examined whether the attachment of cells to the metal plate was required for LPS-induced enhancement of the release of Ni ions. The cells were incubated for 24 h either attached or unattached to the Ni plate, and the concentration of ions released was determined. In the absence of LPS, there was no difference in the release of Ni ions between the attached and unattached cultures (Fig. 9). However, LPS-induced enhancement of the elution was observed when the cells were attached

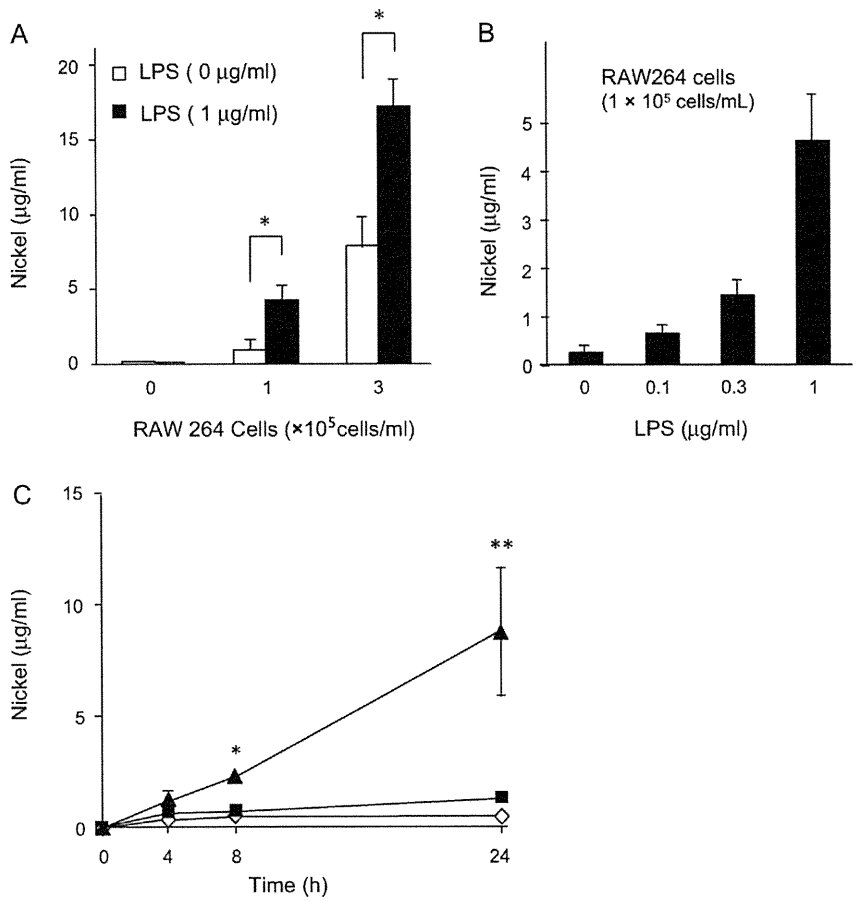

Fig. 7. Enhancement of elution of Ni ions from a Ni plate by LPS-stimulated RAW 264 cells. (A) The cells (1 or 3 × 10^5 cells/ml, 0.2 ml) seeded on a Ni plate (25 mm^2) were incubated for 24 h in the presence (closed columns) or absence (open columns) of LPS (1 μg/ml). The concentration of Ni ions in the supernatant was determined. (B) The cells (1 × 10^5 cells/ml, 0.2 ml) seeded on a Ni plate were incubated for 24 h in medium containing LPS (0.1, 0.3 and 1 μg/ml). (C) The cells (1 × 10^5 cells/ml, 0.2 ml) seeded on a Ni plate were incubated for 4, 8, and 24 h in medium containing LPS (1 μg/ml). Values are the means of five determinations with the S.E.M. shown by vertical bars. Statistical significance: $^{*}P < 0.05$, $^{**}P < 0.01$ vs. the corresponding LPS (0 μg/ml) group.

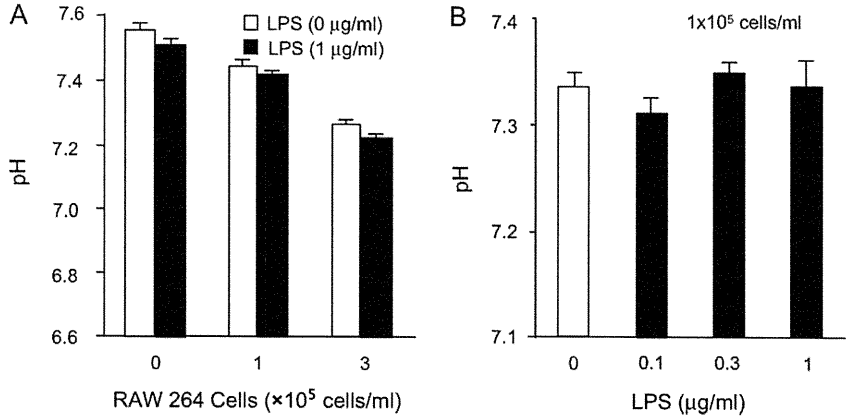

Fig. 8. Changes of pH in the culture medium of LPS-stimulated RAW 264 cells. The cells (1 and 3 × 10^5 cells/ml, 0.2 ml) seeded on a Ni plate (5 mm^2) were incubated for 24 h in the presence (closed columns) or absence (open columns) of LPS (1 μg/ml). The pH of the culture medium was determined with a pH meter. (B) The cells (1 × 10^5 cells/ml, 0.2 ml) seeded on a Ni plate (5 mm^2) were incubated for 24 h in medium containing LPS (0.1, 0.3 and 1 μg/ml). Values are the means for five determinations with the S.E.M. shown by vertical bars.

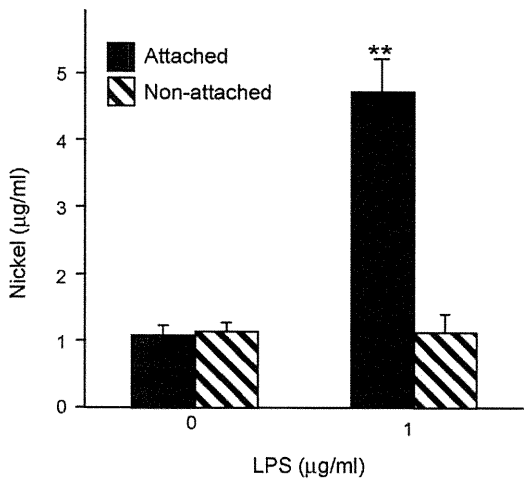

Fig. 9. Requirement of cell attachment for enhancement of the elution of Ni ions from Ni plates by LPS-stimulated RAW 264 cells. The cells (1 × 10^5 cells/ml, 0.2 ml) seeded on (attached condition) or under a Ni plate (non-attached condition) were incubated for 24 h in the presence or absence of LPS (1 μg/ml). The concentration of Ni in the culture medium was determined. Values are the means for five determinations with the S.E.M. shown by vertical bars. Statistical significance: $^{**}P < 0.01$ vs. the corresponding LPS (−) group.

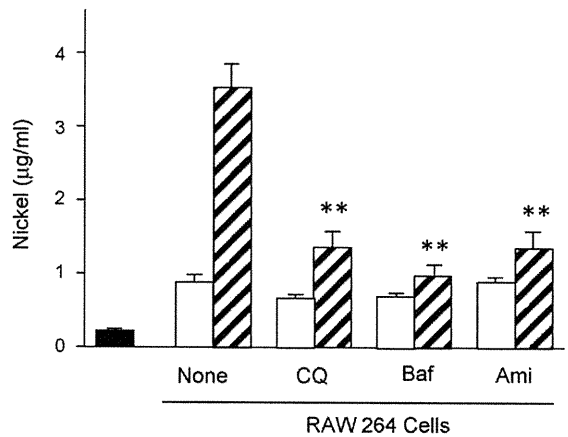

Fig. 10. Effects of inhibitors on the elution of Ni ions from Ni plates by RAW 264 cells. The cells (1 × 10^5 cells/ml, 0.2 ml) were seeded on a Ni plate (5 mm^2) and incubated for 24 h in medium containing chloroquine (CQ; 10 μM), amiloride (Ami; 100 μM) and bafilomycin A_1 (Baf; 1 nM) in the presence (hatched columns) and absence (open columns) of LPS (1 μg/ml). The closed column indicates that the Ni plate was incubated in the medium alone. The concentration of Ni in the supernatant was then determined. Values are the means for five determinations with the S.E.M. shown by vertical bars. Statistical significance: $^{**}P < 0.01$ vs. unstimulated RAW 264 cells, $^{\#\#}P < 0.01$ vs. LPS control.

to the plate (Fig. 9), indicating that the attachment of cells to plate was required to increase the release of Ni ions.

3.9. Effects of inhibitors on the release of Ni ions from the plates

The cells were incubated for 24 h on the Ni plate in the presence of the lysosome inhibitor chloroquine (10 μM), the V-ATPase inhibitor bafilomycin A_1 (1 nM), or the Na^+/H^+ exchanger (NHE) inhibitor amiloride (100 μM), and the concentration of Ni ions in the medium was determined. These inhibitors failed to reduce the release of Ni ions in the absence of LPS, but apparently inhibited it in the presence of LPS (Fig. 10). In the absence of the Ni plate, these inhibitors did not affect the viability of the cells (data not shown). These findings suggested that the release of H^+ by the cells was induced by the stimulation with LPS and caused the release of Ni ions from the plate.

4. Discussion

In this study, using two newly established models to assess the corrosion of Ni *in vivo* and *in vitro*, we found that inflammatory cells accelerated the release of Ni ions from the surface of the metal.

We developed a fluorometric method to determine Ni concentrations in tissue homogenate using Newport Green DCF, an indicator of Zn and Ni ions [17]. The Ni content obtained by the fluorometric assay well correlated with that obtained by ICP-AES, indicating the physiological concentration of Zn ions to be negligible in the fluorometric assay. In this study, we employed wires and plates made of >99% Ni to maximize the release of Ni from alloys. Therefore, the fluorometric assay was a convenient way to determine the concentration of Ni ions. For biomedical alloys such as stainless steel and nitinol, ICP-AES or ICP-MS should be used to assess the release of several metal ions at the same time. Such models are now under investigation.

Interestingly, when the wire was incubated at 37 °C for 8 h in water, saline, or mouse serum, only a little Ni was released. However, Ni ions were released more easily when the wire was implanted subcutaneously in mice, indicating the release to be highly dependent on the activation of cells around the wire. The increase in the concentration of Ni ions around the wire was already evident at 8 h after the implantation and well-correlated with the increase in vascular permeability [14]. Wataha et al. determined the concentration of Ni using a laser-ablation technique in tissue collected 7 days after implantation and demonstrated that the

distribution of the ions correlated well with the extent of necrosis in a Ni wire-implantation model in rats [22]. Therefore, it was likely that the eluted Ni ions caused local inflammation. The finding that the release of Ni ions into tissue was significantly increased by the injection of LPS suggested that the activation of inflammatory cells was involved in the corrosion of the wire. This notion was confirmed *in vitro* using RAW 264 cells. Namely, although little Ni was released from the plate in the medium alone, a significant increase in the elution was elicited in the presence of the cells, and apparently enhanced by the addition of LPS.

This *in vitro* model was useful for clarifying the molecular mechanisms by which activated inflammatory cells elute metals. LPS and inflammatory cytokines such as IL-1 activated V-ATPase and NHE in macrophages [23,24]. The unstimulated cells released a few Ni ions in both attached and unattached cultures and the release was little affected by the three inhibitors. The LPS-enhanced elution of Ni ions was observed only when the cells were attached to the metal and was markedly inhibited by chloroquine, bafilomycin A_1 and amiloride. Similar findings were observed regarding the resorption of bone by osteoclasts [25–27]. Osteoclasts attach to the bone and form a specialized compartment, the sealing zone, in which the resorption of bone is induced. Osteoclasts acidify the space using V-ATPase [28,29]. Because chloroquine neutralizes the acidity and the inhibitor of V-ATPase blocked the acidification, both inhibitors potently suppress bone resorption [30,31]. In addition, the NHE inhibitor also inhibited bone resorption and acidification [32], although the molecular mechanisms involved are not completely clear. However, amiloride inhibits the LPS-induced activation of cells [33,34]. Taken together, the molecular mechanisms of the elution of Ni might be similar to those behind the resorption of bone by osteoclasts. Recently, it was reported that macrophages create the acidic extracellular compartment to aggregated lipoproteins, which was inhibited by bafilomycin A_1 [35]. Thus, macrophages also form the acidic compartment via V-ATPase in various inflammatory processes. These findings suggest that the LPS-stimulated cells on Ni plates form a compartment and acidify it via V-ATPase and NHE, resulting in the elution of Ni ions.

Metal allergy is a concern when using metallic biomedical devices. Since we usually intake Ni ions from foods, the increase in the concentration of Ni ions in plasma might not be enough to induce Ni-allergy. There is a possibility that additional factor such as the exposure to LPS was required to elicit the sensitization of Ni [10]. On the other hand, in the Ni-sensitized persons, the elution of Ni ions from biomedical devices causes Ni-allergy. The most effective way to avoid it is to block the release of metal ions from biomaterials. However, there has been no system to assess the corrosion of metals under inflammatory conditions. We established *in vivo* and *in vitro* models for assessing the release of Ni from metal. In these models, the activation of cells such as macrophages apparently enhanced the corrosion of Ni. Thus, to assess the safety of biomaterials, the release of metal ions under inflammatory conditions should be evaluated. Our models might be useful tools for this purpose. Notably, the *in vitro* model might reflect the elution of Ni at sites of inflammation *in vivo*.

In conclusion, the elution of Ni ions from metal devices was promoted by inflammatory cells attached to the surface and inflammation as well as infection might augment the elution by enhancing the efflux of proton into the sealing zone as is the case for bone resorption.

Acknowledgements

This study was partly supported by Grants-in Aid for Science Research from the Ministry of Health, Labour, and Welfare of Japan, and the Cosmetology Research Foundation.

References

[1] Lee K, Goodman SB. Current state and future of joint replacements in the hip and knee. Expert Rev Med Devices 2008;5:383–93.
[2] Gotman I. Characteristics of metals used in implants. J Endocrinol 1997;11:383–9.
[3] Niinomi M. Metallic biomaterials. J Artif Organs 2008;11:105–10.
[4] Basketter DA, Briatico-Vangosa G, Kaestner W, Lally C, Bontinck WJ. Nickel, cobalt and chromium in consumer products: a role in allergic contact dermatitis? Contact Dermatitis 1993;28:15–25.
[5] Hostynek JJ. Nickel-induced hypersensitivity: etiology, immune reactions, prevention and therapy. Arch Dermatol Res 2002;294:249–67.
[6] Van den Broeke LT, Heffler LC, Linder T, Nilsson JLG, Karlberg AT, Scheynius S. Direct Ni^{2+} antigen formation on cultured human dendritic cells. Immunology 1999;96:578–85.
[7] Thierse HJ, Gamerdinger K, Junkes C, Guerreiro N, Weltzien HU. T cell receptor (TCR) interaction with haptens: metal ions as non-classical haptens. Toxicology 2005;209:101–7.
[8] Artik S, von Vultée C, Gleichmann E, Schwarz T, Griem P. Nickel allergy in mice: enhanced sensitization capacity of nickel at higher oxidation states. J Immunol 1999;163:1143–52.
[9] Artik S, Haarhuis K, Wu X, Begerow J, Gleichmann E. Tolerance to nickel: oral nickel administration induces a high frequency of anergic T cells with persistent suppressor activity. J Immunol 2001;167:6794–803.
[10] Sato N, Kinbara M, Kuroishi T, Kimura K, Iwakura Y, Ohtsu H, et al. Lipopolysaccharide promotes and augments metal allergies in mice, dependent on innate immunity and histidine decarboxylase. Clin Exp Allergy 2007;37:743–51.
[11] Ishii N, Moriguchi N, Nakajima H, Tanaka S, Amemiya F. Nickel sulfate-specific suppressor T cells induced by nickel sulfate in drinking water. J Dermatol Sci 1993;6:159–64.
[12] Ishii N, Sugita Y, Nakajima H, Tanaka S, Askenase PW. Elicitation of nickel sulfate ($NiSO_4$)-specific delayed-type hypersensitivity requires early-occurring and early-acting, $NiSO_4$-specific DTH-initiating cells with an unusual mixed phenotype for an antigen-specific cell. Cell Immunol 1995;161:244–55.
[13] Takeuchi O, Akira S. Toll-like receptors; their physiological role and signal transduction system. Int Immunopharmacol 2001;1:625–35.
[14] Hirasawa N, Goi Y, Tanaka R, Ishihara K, Ohtsu H, Ohuchi K. Involvement of prostaglandins and histamine in nickel wire-induced acute inflammation in mice. J Biomed Mater Res 2010;93A:1306–11.
[15] Zimmerli W. Infection and musculoskeletal conditions: prosthetic-joint-associated infections. Best Pract Res Clin Rheumatol 2006;20:1045–63.
[16] Ochoa RA, Mow CS. Deep infection of a total knee implant as a complication of disseminated pneumococcal sepsis. A case report and review of literature. Knee 2008;15:144–7.
[17] Thierse HJ, Helm S, Pink M, Weltzien H. Novel fluorescence assay for tracking molecular and cellular allergen–protein interactions. J Immunol Methods 2007;328:14–20.
[18] Bowman EJ, Siebers A, Altendorf K. Bafilomycins: a class of inhibitors of membrane ATPase from microorganisms, animal cells, and plant cells. Proc Natl Acad Sci USA 1988;85:7972–6.
[19] De Duve C, De Barsy T, Poole B, Trouet A, Tulkens P, Van Hoof F. Lysosomotropic agents. Biochem Pharmacol 1974;24:2495–531.
[20] Kleyman TR, Cragoe Jr EJ. Amiloride and its analogs as tools in the study of ion transport. J Membr Biol 1988;105:1–21.
[21] Masereel B, Pochet L, Laeckmann D. An overview of inhibitors of Na^+/H^+ exchanger. Eur J Med Chem 2003;38:547–54.
[22] Wataha JC, O'Dell NL, Singh BB, Ghazi M, Whitford GM, Lockwood PE. Relating nickel-induced tissue inflammation to nickel release in vivo. J Biomed Mater Res 2001;58:537–44.
[23] Brisseau GF, Grinstein S, Hackam DJ, Nordström T, Manolson MF, Khine AA, et al. Interleukin-1 increases vacuolar-type H+-ATPase activity in murine peritoneal macrophages. J Biol Chem 1996;271:2005–11.
[24] Vairo G, Royston AK, Hamilton JA. Biochemical events accompanying macrophage activation and the inhibition of colony-stimulating factor-1-induced macrophage proliferation by tumor necrosis factor-α, interferon-γ and lipopolysaccharide. J Cell Physiol 1992;151:630–41.
[25] Shibata T, Amano H, Yamada S, Ohya K. Mechanisms of proton transport in isolated rat osteoclasts attached to bone. J Med Dent Sci 2000;47:177–85.
[26] Evans RW, Cheung HS, McCarty DJ. Cultured human monocytes and fibroblasts solubilize calcium phosphate crystals. Calcif Tissue Int 1984;36:645–50.
[27] Blair HC, Athanasou NA. Recent advances in osteoclast biology and pathological bone resorption. Histol Histopathol 2004;19:189–99.
[28] Henriksen K, Sorensen MG, Jensen VK, Dziegiel MH, Nosjean O, Karsdal MA. Ion transporters involved in acidification of the resorption lacuna in osteoclasts. Calcif Tissue Int 2008;83:230–42.
[29] Xu J, Cheng T, Feng HT, Pavlos NJ, Zheng MH. Structure and function of V-ATPases in osteoclasts: potential therapeutic targets for the treatment of osteolysis. Histol Histopathol 2007;22:443–54.
[30] Kwong CH, Burns WB, Cheung HS. Solubilization of hydroxyapatite crystals by murine bone cells, macrophages and fibroblasts. Biomaterials 1989;10:579–84.
[31] Yao G, Feng H, Cai Y, Qi W, Kong K. Characterization of vacuolar-ATPase and selective inhibition of vacuolar-H(+)-ATPase in osteoclasts. Biochem Biophys Res Commun 2007;357:821–7.

[32] Heming TA, Bidani A. Intracellular pH regulation in U937 human monocytes: roles of V-ATPase and Na^+/H^+ exchange. Immunobiology 2003;207:141–8.
[33] Haddad JJ, Land SC. Amiloride blockades lipopolysaccharide-induced proinflammatory cytokine biosynthesis in an IkB-a/NF-kB-dependent mechanism. Evidence for the amplification of an antiinflammatory pathway in the alveolar epithelium. Am J Respir Cell Mol Biol 2002;26:114–26.
[34] Kamachi F, Ban HS, Hirasawa N, Ohuchi K. Inhibition of lipopolysaccharide-induced prostaglandin E_2 production and inflammation by the Na^+/H^+ exchanger inhibitors. J Pharmacol Exp Ther 2007;321:345–52.
[35] Haka AS, Grosheva I, Chiang E, Buxbaum AR, Baird BA, Pierini LM, et al. Macroophages create an acidic extracellular hydrolytic compartment to digest aggregated lipoproteins. Mol Biol Cell 2009;20:4932–40.

Case Reports in Dermatology

Case Rep Dermatol 2011;3:151–154
DOI: 10.1159/000330731

Published online:
August 9, 2011

ISSN 1662–6567
www.karger.com/cde

Improvement of Cheilitis granulomatosa after Dental Treatment

Ryosuke Sasaki[a] Kayoko Suzuki[b] Teppei Hayashi[c]
Hiroshi Inasaka[d] Kayoko Matsunaga[a]

[a]Department of Dermatology, Fujita Health University School of Medicine, Toyoake, [b]Department of Dermatology, Kariya Toyota General Hospital, Kariya, [c]Ai Dental Office, and [d]Inasaka Clinic, Tokai, Japan

Key Words
Cheilitis granulomatosa · Melkersson-Rosenthal syndrome · Dental infection · Dental metals

Abstract
A 38-year-old male suffered from swelling of the lower lip for 3 months. Neither facial nerve palsy nor fissuring of the tongue was present. Histological examination of a biopsy taken from the lower lip revealed non-caseous epithelioid cell granulomas, suggestive of cheilitis granulomatosa. Patch testing revealed positive reactions to mercury chloride and amalgam. His symptoms markedly improved 3 months after treatment of the apical periodontitis and replacement of dental crowns. As his dental crowns did not contain mercury, we believe that the cheilitis granulomatosa may have been related to the focal dental infection.

Introduction

Cheilitis granulomatosa manifests as edematous swelling of the lips and is considered an incomplete expression of Melkersson-Rosenthal syndrome, a triad of recurrent orofacial edema, recurrent facial nerve palsy and fissuring of the tongue. Various treatments for cheilitis granulomatosa have been reported, but there is no defined treatment for cheilitis granulomatosa. Here, we describe a case of cheilitis granulomatosa that improved after treatment of periodontitis.

Ryosuke Sasaki, MD

Department of Dermatology
Fujita Health University School of Medicine, 1-98 Dengakugakubo
Kutsukake-cho, Toyoake, Aichi 470-1192 (Japan)
Tel. +81 562 95 9256, E-Mail r-sasaki@fujita-hu.ac.jp

Case Rep Dermatol 2011;3:151–154
DOI: 10.1159/000330731
Published online: August 9, 2011

ISSN 1662–6567
www.karger.com/cde

Case Presentation

A 38-year-old male presented with a 3-month history of persistent lower lip swelling (fig. 1). Neither facial nerve palsy nor fissuring of the tongue was present. Previously, he had been treated with antihistamines, 2 weeks minocycline orally, topical corticosteroid and dapsone without success. Laboratory examination revealed no hematologic or biochemical abnormalities. Patch testing showed positive reactions to 0.05% mercury chloride and amalgam (both ++ at D4 according to the ICDRG recommendations). Histopathological findings of a biopsy from the lower lip revealed epithelioid cell granuloma (fig. 2, fig. 3). From the clinical features and histological findings, we diagnosed his condition as cheilitis granulomatosa.

The patient underwent dental treatment to replace his dental metals as he had positively reacted to mercury and amalgam; however, we did not find any mercury in the removed metals. His periodontitis was treated at the same time. Three months after dental treatment, his lip swelling markedly improved.

Discussion

Cheilitis granulomatosa is a rare disease that manifests as a diffuse and painless swelling of the lips. Melkersson-Rosenthal syndrome consists of the triad of recurrent orofacial swelling, relapsing facial paralysis and fissuring of the tongue. Cheilitis granulomatosa is considered an incomplete expression of Melkersson-Rosenthal syndrome [1, 2]. The etiology of cheilitis granulomatosa is unknown, but some cases have been associated with Crohn's disease and sarcoidosis [1–3].

Various treatments for cheilitis granulomatosa have been reported, including antibiotics [4, 5], tranilast [6], oral and intralesional steroids [7, 8], and surgical resection [9]. Rapid improvement and/or complete resolution after dental treatment have been reported [1, 10–12]. Worsaae et al. [1] reported that elimination of the dental infectious foci resulted in regression or disappearance of swelling in 11 out of 16 patients. In our case, there was significant improvement of the lip swelling after treatment of the apical periodontitis and replacement of dental crowns. As the replaced dental crowns did not contain mercury, we believe that our case was associated with periodontitis.

We suggest that examination and treatment of focal dental infections is necessary in the treatment of cheilitis granulomatosa. Cases that do not improve after elimination of dental focal infection [8] require further follow-up.

Case Rep Dermatol 2011;3:151–154
DOI: 10.1159/000330731
Published online: August 9, 2011

ISSN 1662–6567
www.karger.com/cde

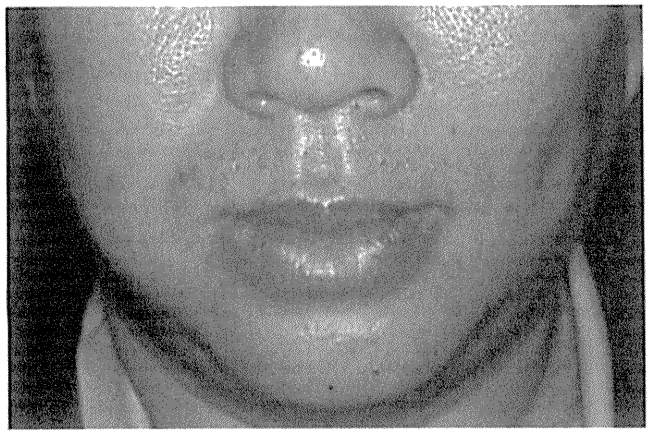

Fig. 1. Clinical appearance at initial presentation showing a marked swelling of the lower lip.

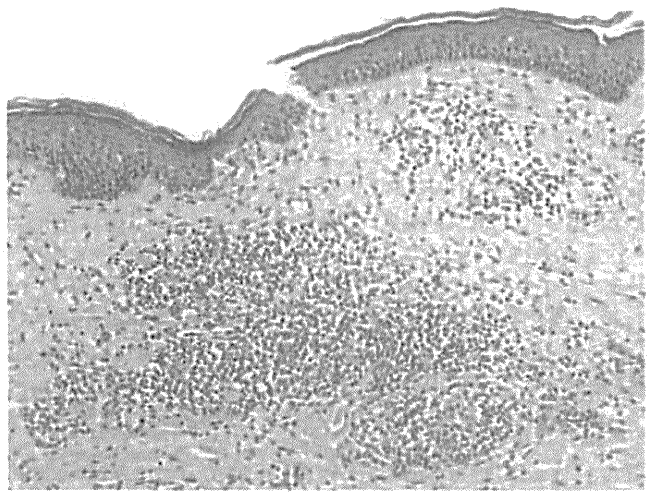

Fig. 2. Histopathology reveals multiple non-caseous epithelioid cell granulomas (HE stain, low magnification).

Case Rep Dermatol 2011;3:151–154
DOI: 10.1159/000330731
Published online: August 9, 2011

ISSN 1662–6567
www.karger.com/cde

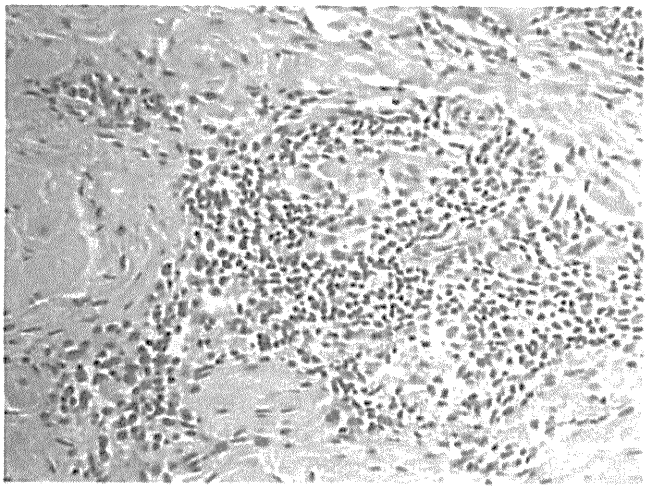

Fig. 3. On higher magnification, non-caseous epithelioid cell granulomas are evident with lymphocytic infiltration (HE stain, high magnification).

References

1 Worsaae N, Cristensen KC, Schiodt M, Reibel J: Melkersson-Rosenthal syndrome and cheilitis granulomatosa. A clinicopathologic study of thirty-three patients with special reference to their oral lesions. Oral Pathol 1982;54:404–413.

2 van der Waal RI, Schulten EA, van der Scheur MR, Wauters IM, Starink TM, van der Waal I: Cheilitis granulomatosa. J Eur Acad Dermatol Venereol 2001;15:519–523.

3 Ratzinger G, Sepp N, Vogetseder W, Tilg H: Cheilitis granulomatosa and Melkersson-Rosenthal syndrome: evaluation of gastrointestinal involvement and therapeutic regimens in a series of 14 patients. J Eur Acad Dermatol Venereol 2007;74:1065–1070.

4 Olivier V, Lacour JP, Castanet J, Perrin C, Ortonne JP: Cheilitis granulomatosa in a child. Arch Pediatr 2000;7:274–277.

5 Inui S, Itami S, Katayama I: Granulomatous cheilitis successfully treated with roxithromycin. J Dermatol 2008;35:244–245.

6 Kato T, Yagami H: Successful treatment of granulomatous cheilitis with tranilast. J Dermatol 1986;13:402–403.

7 Bacci C, Valente ML: Successful treatment of cheilitis granulomatous with intralesional injection of triamcinolone. J Eur Acad Dermatol Venereol 2010;24:363–364.

8 Allen CM, Camisa C, Hamzeh S, Stephens L: Cheilitis granulomatosa: report of six cases and review of literature. J Am Acad Dermatol 1990;23:444–450.

9 Camacho F, García-Bravo B, Carrizosa A: Treatment of Miescher's cheilitis granulomatosa in Melkersson-Rosenthal syndrome. J Eur Acad Dermatol Venereol 2001;15:546–549.

10 Takeshita T, Koga T, Yashima Y: Case repot: cheilitis granulomatosa with periodontitis. J Dermatol 1995;22:804–806.

11 Kawakami T, Fukai K, Sowa J, Ishii M, Teramae H, Kanazawa K: Case of cheilitis granulomatosa associated with apical periodontitis. J Dermatol 2008;35:115–119.

12 Lazarov A, Kidron D, Tulchinsky Z, Minkow B: Contact orofacial granulomatosis caused by delayed hypersensitivity to gold and mercury. J Am Acad Dermatol 2003;49:1117–1120.

ORIGINAL ARTICLE

Topical Cholecystokinin Depresses Itch-Associated Scratching Behavior in Mice

Shoko Fukamachi[1], Tomoko Mori[1], Jun-Ichi Sakabe[1], Noriko Shiraishi[1], Etsushi Kuroda[2], Miwa Kobayashi[1], Toshinori Bito[3], Kenji Kabashima[4], Motonobu Nakamura[1] and Yoshiki Tokura[1,5]

Cholecystokinin (CCK) serves as a gastrointestinal hormone and also functions as a neuropeptide in the central nervous system (CNS). CCK may be a downregulator in the CNS, as represented by its anti-opioid properties. The existence of CCK in the peripheral nervous system has also been reported. We investigated the suppressive effects of various CCKs on peripheral pruritus in mice. The clipped backs of ICR mice were painted with CCK synthetic peptides and injected intradermally with substance P (SP). The frequency of SP-induced scratching was reduced significantly by topical application of sulfated CCK8 (CCK8S) and CCK7 (CCK7S), but not by nonsulfated CCK8, CCK7, or CCK6. Dermal injection of CCK8S also suppressed the scratching frequency, suggesting that dermal cells as well as epidermal keratinocytes (KCs) are the targets of CCKs. As determined using real-time PCR, mRNA for CCK2R, one of the two types of CCK receptors, was expressed highly in mouse fetal skin–derived mast cells (FSMCs) and moderately in ICR mouse KCs. CCK8S decreased *in vitro* compound 48/80-promoted degranulation of FSMCs with a transient elevation of the intracellular calcium concentration. These findings suggest that CCK may exert an antipruritic effect via mast cells and that topical CCK may be clinically useful for pruritic skin disorders.

Journal of Investigative Dermatology (2011) **131,** 956–961; doi:10.1038/jid.2010.413; published online 3 February 2011

INTRODUCTION

Itch or pruritus is an unpleasant cutaneous sensation associated with the immediate desire to scratch (Ikoma *et al.*, 2006; Steinhoff *et al.*, 2006). Histamine was long considered the only mediator of pruritus, but this assumption has changed dramatically in the past two decades. Peripheral itch can be evoked in the skin either directly, by mechanical and thermal stimuli, or indirectly, through chemical mediators (Ikoma *et al.*, 2006). Itch may also be generated in the central nervous system (CNS) independent of peripheral stimulation. Different puritic diseases involved different itch mediators, including histamine, neuropeptides, proteases, prostaglandins, serotonin, acetylcholine, cannabinoids, opioids, bradykinins, cytokines, biogenic amines, neurotransmitters, and ion channels (Steinhoff *et al.*, 2006).

Neuromediators such as neuropeptides and neurotrophins, as well as their receptors, have an important role in peripheral itch. Neuropeptides, as represented by pruritogenic neuropeptide substance P (SP), are produced by sensory nerves, but they can also be elaborated by epidermal keratinocytes (KCs), mast cells, fibroblasts, and other cutaneous immunocompetent cells (Ohkubo and Nakanishi, 1991; Scholzen *et al.*, 1998). Many other mediators are also produced by and secreted from skin-constituent cells in close contact to sensory nerves (Steinhoff *et al.*, 2006). They can activate and sensitize pruritic nerve endings and even modulate their growth, as do nerve growth factors and chemorepellents (Yamaguchi *et al.*, 2008; Yosipovitch and Papoiu, 2008). As for the receptor system, it is notable that KCs, mast cells, and fibroblasts express neurokinin-1 receptor (Ohkubo and Nakanishi, 1991; Scholzen *et al.*, 1998), which is the receptor for SP. These complicated neurophysiological interactions yield itch and render its therapeutic control difficult.

Cholecystokinin (CCK) is a peptide hormone in the gastrointestinal tract (Dufresne *et al.*, 2006), but it also serves as a neuropeptide (Ma *et al.*, 2006). Among neuropeptides, CCKs are most abundantly present in the CNS and involved in numerous physiological functions such as anxiety, depression, psychosis, memory, and feeding behavior (Dufresne *et al.*, 2006). CCKs also have anti-opioid properties in the CNS (Pommier *et al.*, 2002; Mollereau *et al.*, 2005) and exert a nociceptive effect in the spinal cord (Wiesenfeld-Hallin *et al.*, 1999). Furthermore, their existence in the peripheral nervous system has been reported (Moriarty *et al.*, 1997). In various CCKs, sulfation of the tyrosine at position 7

[1]*Department of Dermatology, University of Occupational and Environmental Health, Kitakyushu, Japan;* [2]*Department of Immunology, University of Occupational and Environmental Health, Kitakyushu, Japan;* [3]*Department of Dermatology, Kobe University, Kobe, Japan;* [4]*Department of Dermatology, Kyoto University Graduate School of Medicine, Kyoto, Japan and* [5]*Department of Dermatology, Hamamatsu University School of Medicine, Hamamatsu, Japan*

Correspondence: Yoshiki Tokura, Department of Dermatology, Hamamatsu University School of Medicine, 1-20-1 Handayama, Higashi-Ku, Hamamatsu 431-3192, Japan. E-mail: tokura@hama-med.ac.jp

Abbreviations: CCK, cholecystokinin; CCK2R, CCK2 receptor; CCK7S, sulfated CCK7; CCK8S, sulfated CCK8; CNS, central nervous system; FSMC, murine fetal skin–derived mast cell; KC, keratinocyte; SP, substance P

Received 15 February 2010; revised 3 November 2010; accepted 12 November 2010; published online 3 February 2011

from the C-terminus is a posttranslational modification that makes them biologically active peptides (Ma *et al.*, 2006). Varying lengths of CCKs with or without sulfate have been studied for their activities as gastrointestinal hormones (Bonetto *et al.*, 1999) and as CNS players (Rehfeld *et al.*, 2007). Two types of CCK receptors have been identified: CCK1R (CCK-A receptor) and CCK2R (CCK-B receptor). CCK1R usually requires sulfated CCKs. CCK2R affords a binding site to both sulfated and nonsulfated ligands, but nonsulfated CCKs have affinities that are decreased 10- to 50-fold (Dufresne *et al.*, 2006). CCKs exert their biological functions by interacting with CCK receptors located on multiple target cells in the CNS and on peripheral nerve endings (Dufresne *et al.*, 2006; Rehfeld *et al.*, 2007; Zheng *et al.*, 2009). In the brain, sulfated CCK8 (CCK8S) is most abundant (Rehfeld *et al.*, 2007) and possesses one of the strongest endogenous anti-opioid properties (Ma *et al.*, 2006). Prolonged opioid exposure increases the expression of CCKs and CCK2R in the CNS, where CCK8S negatively modulates opioid responses and maintains homeostasis of the opioid system (Pommier *et al.*, 2002; Agnes *et al.*, 2008). Thus, it seems that CCKs are downregulators of opioid-mediated pruritus in CNS. However, the function of CCKs, the distribution of CCK receptors in the skin, and their effects on peripheral pruritus remain unelucidated (Ma *et al.*, 2006).

In this study, we investigated the antipruritic effects of different lengths of CCKs with or without sulfate, which were topically applied onto the skin of mice. Results suggest that CCKs are capable of reducing SP-induced scratching at least by affecting the function of mast cells. Our findings may lead to the development of previously unreported antipruritic strategies.

RESULTS

Depressive effects of topical application of CCKs on SP-induced itch-associated response

We tested various CCKs for their ability to suppress scratching behavior induced by intradermal SP injection in ICR mice (Andoh *et al.*, 2001). We first examined the effect of percutaneously applied CCK on the response. Because CCK8S has an inhibitory ability in the CNS (Pommier *et al.*, 2002; Dufresne *et al.*, 2006) and gastrointestinal tract (Miyasaka *et al.*, 2004), CCK8S and the other CCK constructs consisting of smaller amino acids with or without sulfate (Table 1) were tested for their antipruritic activities. ICR mice were painted with various CCKs on the clipped, tape-stripped rostral part of the back skin ($\sim$1.8 cm^2) and then injected with SP intradermally at the CCK-painted site.

The topical application of CCK8S significantly reduced the scratching frequency, as compared with the nonapplied control (Figure 1a). Sulfated CCK7 (CCK7S) also reduced the scratching frequency, to a level comparable to that with CCK8S, whereas nonsulfated CCK8, CCK7, and CCK6 had no ability to suppress scratching. These results showed that CCKs have an antipruritic ability, and CCK constructs bearing sulfation of position 7 are required for the ability to suppress the scratching behavior. In this itch-associated-scratching model, we also administered CCK8S intradermally together with SP to mice. The scratching frequency induced by SP was profoundly suppressed by the simultaneous injection of CCK8S (Figure 1b). When the time course of effects induced by CCK8S was examined, both topical application (Figure 1c) and intradermal injection (Figure 1d) of CCKS reduced the scratching frequency at intervals of 0–5 minutes and 5–10 minutes.

These findings raised the possibility that epidermal and dermal cells participating in the development of itch are affected by CCKs.

Table 1. Amino acid sequences of CCK and its constructs

Sulfated CCK8 (CCK8S)	Asp–Tyr (SO_3–)–Met–Gly–Trp–Met–Asp–Phe–NH_2
Nonsulfated CCK8 (CCK8)	Asp–Tyr–Met–Gly–Trp–Met–Asp–Phe–NH_2
Sulfated CCK7 (CCK7S)	Tyr (SO_3–)–Met–Gly–Trp–Met–Asp–Phe–NH_2
Nonsulfated CCK7 (CCK7)	Tyr–Met–Gly–Trp–Met–Asp–Phe–NH_2
Nonsulfated CCK6 (CCK6)	Met–Gly–Trp–Met–Asp–Phe–NH_2

Abbreviation: CCK, cholecystokinin.

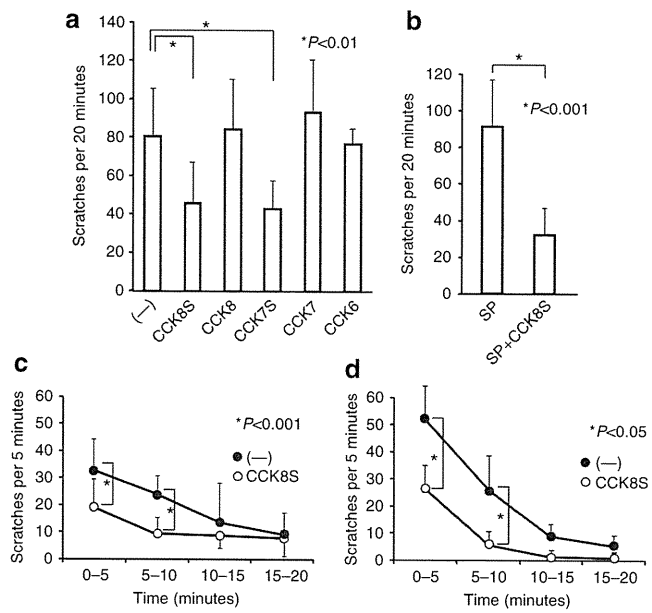

Figure 1. Suppression of substance P (SP)-induced itch by percutaneous application or intradermal injection of cholecystokinins (CCKs). (**a**) ICR mice were painted on the clipped skin with CCKs (0.5 nmol per site) and injected intradermally with SP (100 nmol per site). The group depicted with "(—)" represents mice injected with vehicle (acetone/olive oil) alone. The numbers of mice were as follows: CCK (—), $n=12$; CCK8S, $n=10$; CCK8, $n=6$; CCK7S, $n=6$; CCK7, $n=3$; and CCK6, $n=4$. (**b**) ICR mice were injected intradermally with SP or with SP and CCK8S. Each bar represents the mean of scratches per 20 minutes. CCK (—), $n=5$ and CCK8S, $n=8$. (**c**) Time course of scratching frequency in mice untreated ($n=12$) or topically administered CCK8S ($n=10$). (**d**) Time course of scratching frequency in mice untreated ($n=5$) or intradermally injected with CCK8S ($n=8$). CCK7, nonsulfated CCK7; CCK8, nonsulfated CCK8; CCK7S, sulfated CCK7; CCK8S, sulfated CCK8.

CCK2R expression in KCs and mast cells

Both KCs and mast cells are the possible targets of CCKs in the suppression of SP-induced pruritus. It is known that KCs express the receptors for itch-related molecules, neurokinin-1 receptor for SP, H1 receptor for histamine, and protease-activated receptor-2 for tryptase (synthetic agonist, SLIGRL-NH_2). Mast cells are well known to possess neurokinin-1 receptor (Scholzen *et al.*, 1998; Liu *et al.*, 2006). We investigated the expression of the CCK receptors CCK1R and CCK2R in KCs and mast cells. Primary cultures of KCs from ICR mice and fetal skin-derived mast cells (FSMCs) were collected, and mRNAs for CCK1R and CCK2R were quantitated by real-time PCR, RT-PCR, and western blotting analyses. The two types of cells expressed both CCK1R and CCK2R at the mRNA and protein levels (Figure 2). When the expression levels of real-time PCR analysis were normalized with the β-actin level, the two receptors were more highly expressed in FSMCs than in KCs.

In a preliminary DNA microarray analysis of normal human epidermal KCs, we investigated the levels of gene expression from stimulation with SP (10^{-6} M), histamine (10 μg ml^{-1}), or SLIGRL-NH_2 (100 nM) under high calcium (0.6 mM) concentration. The CCK2R expression by SP-stimulated KCs was most elevated; its level was $2^{8.67}$ times that of the control (Supplement Data online). Such an increased CCK2R expression was not observed with histamine or SLIGRL-NH_2. This observation suggested that CCK2R has an important role in the suppression of SP-stimulated KCs. To determine the effect of SP on KCs, ICR mouse KCs were incubated with SP for 30 minutes to 24 hours, and the expression of CCK2R and CCK1R was analyzed by western blotting. CCK2R was detected with antibodies as a 78 kDa band (Morisset *et al.*, 2003) and increased in KCs exposed to SP for 5 or 6 hours (Figure 3a). By contrast, CCK1R expression was not augmented by SP (Figure 3b). Thus, the expression of some receptors for CCK is enhanced by SP, depending on the receptor.

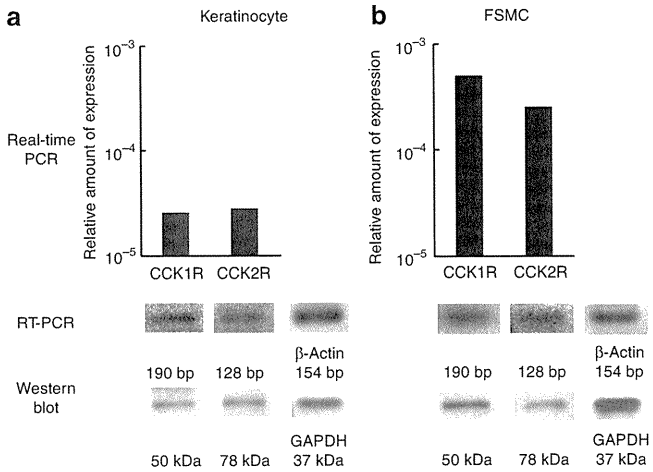

Figure 2. CCK-A receptor (CCK1R) and CCK-B receptor (CCK2R) mRNA expression in keratinocytes and mast cells. Cultured ICR mouse keratinocytes (**a**) and fetal skin-derived mast cells (FSMCs) (**b**) were examined for the expression of mRNAs for CCK1R and CCK2R using real-time PCR and RT-PCR and for the expression of their proteins using western blotting analysis. Data are expressed as the amount of expression relative to β-actin. Glyceraldehyde-3-phosphate dehydrogenase (GAPDH) was used as control for western blotting.

Suppression of FSMC degranulation by CCK8S with transient elevation of intracellular calcium

The above findings suggested that CCKs bind to CCK2R on KCs and mast cells and downmodulate their itch-related biological functions. Given that the level of CCK2R expression was higher in FSMCs than in KCs and the application of CCKs immediately exerted its inhibitory effects on the scratching behavior, it is possible that CCKs directly affect mast cells. We therefore focused on mast cells as the primary target. The addition of compound 48/80 induced degranulation of FSMCs (Figure 4a). This promoted degranulation of FSMCs, which was significantly inhibited by CCK8S at 10^{-8} or 10^{-7} M concentration.

To test whether CCK8S evokes signal transduction in mast cells, we measured the intracellular calcium using confocal recording. The fluorescence intensity of 15 cells positively responding on addition of CCK8S was monitored with computerized color change on a display using a digital image processing system. The mast cells exhibiting green fluorescence of Fluo-4-AM at any time point between 40 and

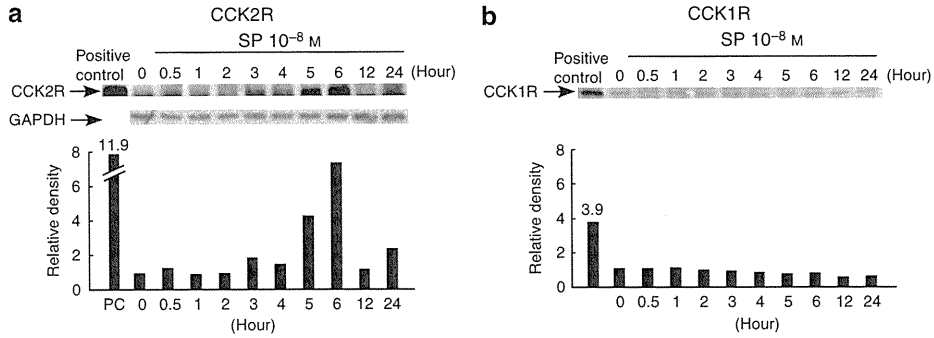

Figure 3. Western blotting of CCK-A receptor (CCK1R) and CCK-B receptor (CCK2R) in mouse keratinocytes stimulated with substance P (SP). ICR mouse keratinocytes were incubated with SP (10^{-8} M) for 0.5–24 hours and harvested at each time point. The expression levels of CCK2R (**a**) and CCK1R (**b**) were analyzed by western blotting. NIH/3T3 whole lysates were used as positive control. Glyceraldehyde-3-phosphate dehydrogenase (GAPDH) was used as control for western blotting and exhibited similar intensities in the samples cultured for 0–24 hours. The intensity of each band was subjected to densitometric analysis and expressed as density relative to the nontreated control (0).

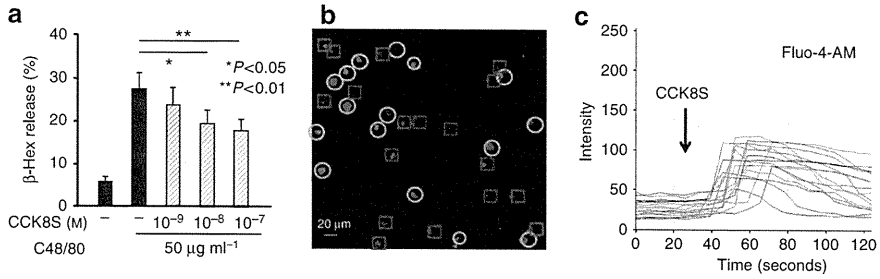

Figure 4. Suppression of fetal skin-derived mast cell (FSMC) degranulation by sulfated CCK8 (CCK8S) with transient intracellular calcium increase. (**a**) FSMCs were incubated with or without CCK8S in the presence of compound 48/80 (C48/80; 50 μg ml^{-1}) for 15 minutes. Supernatants and cell lysates were incubated with *p*-nitrophenyl-*N*-acetyl-β-D-galactosaminide, and β-hexosaminidase (β-Hex) release was determined as the ratio between activity in the supernatant and cell lysate, multiplied by 100. (**b**) FSMCs were loaded with Fluo-4-AM (green) and stained for CD117 (c-kit, red). The percentage of CCK8S-responding FSMCs was determined from the fluorescence traces of all cells. Circles represent responding FSMCs and squares represent nonresponding FSMCs. Bar = 20 μm. (**c**) The addition of CCK8S to FSMC culture induced an increase in intracellular calcium level.

80 seconds after CCK8S addition were defined as positively responding cells (Figure 4b and c); these are marked with a yellow circle in Figure 4b. The addition of CCK8S to the FSMC culture induced a prompt rise of calcium that persisted for more than 2 minutes and then gradually declined, indicating that CCK8S induces signaling via CCK2R in mast cells. The percentage of responding FSMCs was determined from the fluorescence traces of all cells. As shown in Figure 4b, in which circles and squares represent CCK8S-responding and nonresponding FSMCs, respectively, 45% (16 of 36 cells) of FSMCs were typically activated by CCK8S.

DISCUSSION

Despite their original name of cholecyst stimulators, CCKs have been known to serve as CNS modulators (Dufresne *et al.*, 2006) and CCK8S downmodulates opioid responses (Pommier *et al.*, 2002; Agnes *et al.*, 2008). As suggested in our present study, CCKs may also have a function of downmodulator in the peripheral itch. The topical application of CCKs suppressed the itch-related scratching behavior evoked by SP injection. The expression of CCK2R, but not CCK1R, in murine and human KCs was markedly enhanced by exposure to SP. It is likely that CCK2R, whose expression is augmented by SP, has a down-regulatory role in the excess peripheral itch.

Among the CCK constructs consisting of different numbers of amino acids with or without sulfate, CCK8S and CCK7S, but not CCK8, CCK7, or CCK6, exerted an antipruritic action. Therefore, in a comparison between CCK8S and CCK8 and between CCK7S and CCK7, sulfation of position 7 is required for the ability to suppress the scratching behavior. This is in accordance with the observation that CCK8S has an anxiogenic effect (Harro, 2006), a depressant effect, and an anti-opioid effect (Noble *et al.*, 1999), but the effects of CCK are limited by desulfation of the tyrosine (Tokunaga *et al.*, 1993).

Although the exact mode of antipruritic action of CCKs is still speculative, some informative observations were obtained from the study. Both percutaneous application and dermal injection were effective routes for CCK8S in suppressing itch, suggesting that epidermal and/or dermal constituents are the targets of CCKs. Furthermore, the administration of CCK8S rapidly inhibited the SP-induced itch. We thus investigated the mechanism of CCK suppression of itch in *in vitro* studies, focusing on mast cells. CCK8S significantly reduced the degranulation of FSMCs with elevation of intracellular calcium concentration, suggesting that mast cell degranulation is inhibited by CCK8S through CCK2R. Alternatively, or additionally, KCs are possibly involved in CCR action. KCs are thought to mediate pruritus by releasing inflammatory mediators and neurotrophins. Therefore, the antipruritic effect of CCK8S on KCs, if any, seems to need a time lag to operate. As the therapeutic action of topical CCK8S is rapid, mast cells may be more likely targeted by CCK8S than KCs. The high expression of CCK2R in mast cells further supports the notion that mast cells are sensitive to CCKs. However, SP was reported to cause scratching behavior in both mast cell–deficient and wild-type mice (Hossen *et al.*, 2003), suggesting a mast cell-independent mechanism of SP-evoked itch. Given this observation, it is possible that another skin constituent, such as the sensory nerves, is affected by CCKs. The target cells and the actions of CCK8S on them warrant elucidation in the future.

The antipruritic effects of CCK8S and CCK7S on this mouse itch model may afford a therapeutic use for the CCKs for the treatment of skin diseases with peripheral itch. Given that the major target of CCKs is mast cells, urticaria, atopic dermatitis, contact dermatitis, and other types of eczematous dermatitis would be successfully treated with CCKs topically applied to the skin. The therapeutic effects of CCKs on peripheral itch may shed light on the mechanisms underlying the physiological regulation of itch, and it is notable that CCKs have potential as a topical drug for pruritic skin diseases.

MATERIALS AND METHODS

Animals

Female ICR mice were obtained from KBT Oriental (Tosu, Japan). These mice were maintained in the Laboratory Animal Research Center of the University of Occupational and Environmental Health under specific-pathogen-free conditions and used at the age of 6–8 weeks. All animal experiments were performed according to the guidelines approved by our university for the care and use of animals.

Reagents

SP, CCK8S, nonsulfated CCK8, CCK7S, and nonsulfated CCK6 were purchased from the Peptide Institute (Osaka, Japan). Nonsulfated

CCK7 was purchased from Funakoshi (Tokyo, Japan). Compound 48/80 was purchased from Sigma (St Louis, MO).

Itch-associated scratching behavior and topical application of CCKs

The hair was clipped over the rostral part of the each mouse's back 1 or 2 days before the experiment. Before behavioral recording, each animal (four per observation) was put into an acrylic cage (18 × 23 × 11 cm) for at least 1 hour for acclimation. An intradermal injection of SP (100 nmol in 50 µl of physiological saline per site) induced scratching of the skin around the injected site with the hindpaws (Andoh *et al.*, 2001). CCKs were topically applied in two ways: percutaneous application and intradermal injection. For percutaneous application, the shaved back skin was stripped with Scotch tape (3 M) six times on the day before the experiment (Nishijima *et al.*, 1997). The clipped backs of the mice were painted (1.8 cm^2, 1.5 cm in diameter) with 20 µl CCK (0.5 nmol per site) in acetone/olive oil (3:1) 3–4 minutes before the SP injection (100 nmol per site). For intradermal application, mice were injected intradermally with CCK (0.5 nmol per site in 20 µl physiological saline), followed immediately by SP injection at the same site (100 nmol per site). Immediately after treatment, the animals were put back into the same cage and their behavior was videotaped for 40 minutes using a digital video camera (Andoh *et al.*, 2001). Using the video, the frequency of scratching toward the injected site by the hindpaws was recorded for the first 20 minutes.

Murine KCs

The skin of ICR newborn mice was peeled within 24 hours after birth and incubated with 0.05% collagenase (collagenase from *Clostridium histolyticum* type 2; Sigma) for 2 days at 37 °C in a 5% CO_2 atmosphere. Epidermal sheets were collected and suspended in culture medium. Cell suspension was plated into six-well plates (Corning Glass Works, Corning, NJ) and grown to subconfluence in CnT-07 medium (Funakoshi).

Murine mast cells

The method for preparation of murine FSMCs has been described previously (Yamada *et al.*, 2003). Day 14 fetal skin was dissociated by 0.25% trypsin for 20 minutes at 37 °C in Hank's balanced salt solution (Gibco, Carlsbad, CA). Erythrocytes were lysed using RBC-lysing buffer (Sigma) and, after washing, cells were resuspended in complete RPMI, which is RPMI-1640 (Gibco) supplemented with 5% fetal bovine serum (Gibco), 1% nonessential amino acids (Gibco), 1% sodium pyruvate (Gibco), antibiotic/antimycotic (Invitrogen, Carlsbad, CA), and 0.1% 2-mercaptoethanol (Gibco). Fifty milliliters of the cell suspension in each 175 cm^2 75-flask (Corning Glass Works) was cultured in the presence of 20 ng ml^{-1} recombinant mouse IL-3 (Invitrogen) and 20 ng ml^{-1} recombinant mouse stem cell factor (Biosource, Camarillo, CA) at 37 °C without changing the medium. Nonadherent and loosely adherent cells were harvested. The cells were centrifuged and resuspended in RPMI, layered on 40% Percoll (GE Healthcare, Buckinghamshire, England), and centrifuged at room temperature. The cell pellet at the bottom was used as FSMCs. For flowcytometric analysis, cells were stained with phycoerythrin-conjugated anti-mouse FcεRI (eBioscience, San Diego, CA) and Alexa Fluor 700-conjugated anti-mouse CD117 (c-kit; eBioscience) for 20 minutes on ice, washed twice, and then resuspended with FACS buffer. Flow cytometric analysis was performed with FACS Canto (BD, Franklin Lakes, NJ) and FlowJo software (TreeStar, San Carlos, CA). The purity of FSMCs was 95%, as determined by both FcεRI and CD117 positivity by flow cytometry.

Real-time quantitative RT-PCR analysis

Total RNA was extracted from the cell pellet using the PureLink RNA Mini Kit (Invitrogen). cDNA was reverse transcribed from total RNA samples using the TaqMan Reverse Transcription reagents (Applied Biosystems, Carlsbad, CA). mRNA expression was quantified by real-time PCR using SYBR Green Dye (PE Biosystems, Foster City, CA) with an ABI PRISM 7000 Sequence Detection System (Applied Biosystems) according to the manufacturer's instructions. Primers were designed using Primer Bank for the human and murine genes, and they were constructed by Invitrogen. The sequences are as follows: murine β-actin: 5′-GGCTGTATTCCCCTCCATCG-3′ and 5′-CCAGTTGGTAACAATGCCATGT-3′; murine CCK2R: 5′-GATGG CTGCTACGTGCAACT-3′ and 5′-CGCACCACCCGCTTCTTAG-3′; and murine CCK1R: 5′-CACGCTGGTTATCACGGTG-3′ and 5′-GC CCATGAAGTAGGTGGTAGTC-3′. The conditions for the real-time PCR were as follows: 2.0 minutes at 50 °C, 10 minutes at 95 °C, and then 50 cycles of amplification consisting of 15 seconds at 95 °C and 1 minute at 60 °C. All heating and cooling steps were performed with a slope of 20 °C per second. Relative expression was calculated using the delta Ct method.

Western blotting

KCs from ICR mice were stimulated with SP (10^{-8} M) in six-well plates (Corning Glass Works) for 0.5–24 hours, harvested with a rubber policeman, and subjected to extraction with RIPA buffer (Wako, Osaka, Japan; 50 mM Tris-HCl (pH8.0), 150 mM sodium chloride, 0.5% (wt/vol) sodium deoxycholate, 0.1% (wt/vol) SDS, and 1.0% (wt/vol) NP-40 substitute). Protein samples (20 ìg) were separated by 8% SDS-polyacrylamide gel electrophoresis and electroblotted onto polyvinylidene difluoride membranes for 2 hours at 180 mA. After blocking with 5% skim milk solution, the membranes were incubated with rabbit anti-mouse CCK1R (SC-33220; 1:1,000, Santa Cruz, Santa Cruz, CA), CCK2R (SC-33221; 1:1,000, Santa Cruz) polyclonal antibodies, or GAPDH (SC-25887; 1:1,000, Santa Cruz), and the reaction was detected with horseradish peroxidase-conjugated goat anti-rabbit IgG (1:3,000, Bio-Rad, Hercules, CA). Immunoblots were visualized using the ECL Plus Western Blotting Detection Reagents (GE Healthcare) according to the manufacturer's protocol. Bands were quantified by densitometry with the help of a CS Analyzer version 2.0 (ATTO, Tokyo, Japan). NIH/3T3 whole cell lysate (Santa Cruz) was used as a positive control.

Mast cell degranulation

Degranulation of FSMCs was assessed by β-hexosaminidase assay (Yamada *et al.*, 2003; Noguchi *et al.*, 2005). FSMCs were washed with Tyrode's buffer (Sigma) and resuspended at a concentration of 2×10^4 cells per well into a 96-well plate. FSMCs were incubated with or without CCK8S in the presence of compound 48/80 (50 µg ml^{-1}) for 15 minutes at 37 °C. The plate was centrifuged for 5 minutes, and the supernatants were placed into another 96-well plate. Cell pellets were resuspended in Tyrode's buffer containing 0.5% triton X-100 (Sigma). Supernatants and cell lysates (50 µl) were incubated with 100 µl of 2.5 mM *p*-nitrophenyl-*N*-acetyl-β-D-galactosaminide (Sigma),

dissolved in 0.04 mM citrate buffer (pH 4.5), at 37 °C for 90 minutes. The reaction was stopped with 100 µl of 0.4 M glycine (pH 10.7; MP Biomedicals, Solon, OH). The plate was read at 405 nm using a 595 nm reference filter in a microplate reader (Bio-Rad). β-Hexosaminidase release was determined as the ratio between activity in the supernatant and the cell lysate, multiplied by 100.

Calcium influx determined by confocal imaging

Confocal imaging of cells loaded with fluorescent dyes was performed using a Zeiss LSM5 pascal (Carl Zeiss, Jena, Germany). FSMCs were loaded with Fluo-4-AM (Invitrogen; 1 µM) at 37 °C for 20 minutes, washed twice, and set aside for at least 40 minutes. FSMCs were also stained for CD117 (c-kit) with Alexa Fluor 700–conjugated anti-mouse CD117 antibody. The LSM5 multitrack configuration was used for simultaneous measurement of intracellular calcium concentration (excitation, 488 nm; emission, long-pass 505 nm filter) and the expression of CD117 (excitation, 633 nm; emission, long-pass 650 nm filter). Images were recorded (usually recording for 300 seconds) at room temperature, in a 512 × 512-pixel format. As stimulants, SP or CCKs were added directly to the bath as a small drop (10 µl; final concentration, 10^{-6} M SP and 10^{-6} M CCK8S). Image data were analyzed offline using the Zeiss LSM510 analyzing software (LSM Image Examiner, Carl Zeiss). The mast cells exhibiting green fluorescence of Fluo-4-AM at any time point between 40 and 80 seconds after CCK8S addition were defined as positively responding cells.

Gene-array analysis

Normal human epidermal KCs were cultured with SP (10^{-6} M), histamine (10 mg ml^{-1}), and SLIGRL-NH_2 (100 nM) for 2 hours and harvested. For DNA microarray analysis, total RNA was extracted from Normal human epidermal KCs with the RNeasy Mini Kit (Qiagen, Valencia, CA). Images were analyzed with the DNASIS Array (DNA Chip Research, Hitachi Software Engineering, Tokyo, Japan) according to the manufacturer's instructions. The results of DNA microarray analysis of the top and bottom 20 genes with respect to expression levels induced by SP, histamine, or SLIGRL-NH_2 are shown in the Supplementary Data online.

Statistical analysis

Data were analyzed using an unpaired Student's *t*-test. $P<0.05$ was considered to be significant.

CONFLICT OF INTEREST

The authors state no conflict of interest.

ACKNOWLEDGMENTS

This study was supported by a grant from the Ministry of Education, Science, Sports and Culture and a grant from the Ministry of Health, Labour and Welfare, Japan. We thank Yukako Miyazaki and Rie Murase for their technical assistance.

SUPPLEMENTARY MATERIAL

Supplementary material is linked to the online version of the paper at http://www.nature.com/jid

REFERENCES

Agnes RS, Ying J, Kover KE *et al.* (2008) Structure-activity relationships of bifunctional cyclic disulfide peptides based on overlapping pharmacophores at opioid and cholecystokinin receptors. *Peptides* 29:1413–23

Andoh T, Katsube N, Maruyama M *et al.* (2001) Involvement of leukotriene B(4) in substance P-induced itch-associated response in mice. *J Invest Dermatol* 117:1621–6

Bonetto V, Jornvall H, Andersson M *et al.* (1999) Isolation and characterization of sulphated and nonsulphated forms of cholecystokinin-58 and their action on gallbladder contraction. *Eur J Biochem* 264:336–40

Dufresne M, Seva C, Fourmy D (2006) Cholecystokinin and gastrin receptors. *Physiol Rev* 86:805–47

Harro J (2006) CCK and NPY as anti-anxiety treatment targets: promises, pitfalls, and strategies. *Amino Acids* 31:215–30

Hossen MA, Sugimoto Y, Kayasuga R *et al.* (2003) Involvement of histamine H3 receptors in scratching behaviour in mast cell-deficient mice. *Br J Dermatol* 149:17–22

Ikoma A, Steinhoff M, Ständer S *et al.* (2006) The neurobiology of itch. *Nat Rev Neurosci* 7:535–47

Liu JY, Hu JH, Zhu QG *et al.* (2006) Substance P receptor expression in human skin keratinocytes and fibroblasts. *Br J Dermatol* 155:657–62

Ma KT, Si JQ, Zhang ZQ *et al.* (2006) Modulatory effect of CCK-8S on GABA-induced depolarization from rat dorsal root ganglion. *Brain Res* 1121:66–75

Miyasaka K, Ohta M, Kana S *et al.* (2004) Enhanced gastric emptying of a liquid gastric load in mice lacking cholecystokinin-B receptor: a study of CCK-A,B,and AB receptor gene knockout mice. *J Gastroenterol* 39:319–23

Mollereau C, Roumy M, Zajac JM (2005) Opioid-modulating peptides: mechanisms of action. *Curr Top Med Chem* 5:341–55

Moriarty P, Dimaline R, Thompson DG *et al.* (1997) Characterization of cholecystokininA and cholecystokininB receptors expressed by vagal afferent neurons. *Neuroscience* 79:905–13

Morisset J, Julien S, Lainé J (2003) Localization of cholecystokinin receptor subtypes in the endocine pancreas. *J Histochem Cytochem* 51:1501–13

Nishijima T, Tokura Y, Imokawa G *et al.* (1997) Altered permeability and disordered cutaneous immunoregulatory function in mice with acute barrier disruption. *J Invest Dermatol* 109:175–82

Noble F, Wank SA, Crawley JN *et al.* (1999) International union of Pharmacology. XXI. Structure, distribution, and functions of cholecystokinin receptors. *Pharmacol Rev* 51:745–81

Noguchi J, Kuroda E, Yamashita U (2005) Strain difference of murine bone marrow-derived mast cell functions. *J Leukoc Biol* 78:605–11

Ohkubo H, Nakanishi S (1991) Molecular characterization of the three tachykinin receptors. *Ann NY Acad Sci* 632:53–62

Pommier B, Beslot F, Simon A *et al.* (2002) Deletion of CCK2 receptor in mice results in an upregulation of the endogenous opioid system. *J Neurosci* 22:2005–11

Rehfeld JF, Friis-Hansen L, Goetze JP *et al.* (2007) The biology of cholecystokinin and gastrin peptides. *Curr Top Med Chem* 7:1154–65

Scholzen T, Armstrong CA, Bunnett NW *et al.* (1998) Neuropeptides in the skin: interactions between the neuroendocrine and the skin immune systems. *Exp Dermatol* 7:81–96

Steinhoff M, Bienenstock J, Schmelz M *et al.* (2006) Neurophysiological, neurological, and neuroendocrine basis of pruritus. *J Invest Dermatol* 126:1705–18

Tokunaga Y, Cox KL, Coleman R *et al.* (1993) Characterization of cholecystokinin receptors on the human gall bladder. *Surgery* 113:155–62

Wiesenfeld-Hallin Z, de Araúja Lucas G, Alster P *et al.* (1999) Cholecystokinin/opioid interactions. *Brain Res* 848:78–89

Yamada N, Matsushima H, Tagaya Y *et al.* (2003) Generation of a large number of connective tissue type mast cells by culture of murine fetal skin cells. *J Invest Dermatol* 121:1425–32

Yamaguchi J, Nakamura F, Aihara M *et al.* (2008) Semaphorin3A alleviates skin lesions and scratching behavior in NC/Nga mice, an atopic dermatitis model. *J Invest Dermatol* 128:2842–9

Yosipovitch G, Papoiu AD (2008) What causes itch in atopic dermatitis? *Curr Allergy Asthma Rep* 8:306–11

Zheng Y, Akgun E, Harikumar KG *et al.* (2009) Induced association of mu opioid (MOP) and type 2 cholecystokinin (CCK2) receptors by novel bivalent ligands. *J Med Chem* 52:247–58

Journal of Dermatological Science 61 (2011) 118–123

Contents lists available at ScienceDirect

Journal of Dermatological Science

journal homepage: www.elsevier.com/jds

Modulation of semaphorin 3A expression by calcium concentration and histamine in human keratinocytes and fibroblasts

Shoko Fukamachi [a], Toshinori Bito [b], Noriko Shiraishi [a], Miwa Kobayashi [a], Kenji Kabashima [c], Motonobu Nakamura [a], Yoshiki Tokura [a,*]

[a] Department of Dermatology, University of Occupational and Environmental Health, Iseigaoka, Yahatanishi-ku, Kitakyushu 807-8555, Japan
[b] Division of Dermatology, Department of Internal Related, Kobe University Graduate School of Medicine, Kobe, Japan
[c] Deparment of Dermatology, Faculty of Medicine, Kyoto University Graduate School of Medicine, Kyoto, Japan

ARTICLE INFO

Article history:
Received 30 April 2010
Received in revised form 27 October 2010
Accepted 23 November 2010

Keywords:
Semaphorin 3A
Nerve growth factor
Keratinocyte
Calcium concentration
Histamine
PAR-2

ABSTRACT

Background: Both neurotrophins and chemorepellents are involved in the elongation and sprouting of itch-associated C-fibers in the skin. Nerve growth factor (NGF) and semaphorin 3A (Sema3A) are representatives of these two types of axon-guidance factors, respectively.
Objective: We investigated the effects of calcium concentration and histamine on the expression of NGF and Sema3A in normal human epidermal keratinocytes (NHEK) and normal human fibroblasts (NHFb).
Methods: NHEK and NHFb were cultured under different calcium concentrations (0.15–0.9 mM) with or without histamine, and the expression of mRNA for *NGF* and *SEMA3A* was assessed by real-time PCR analysis. An immunohistochemical study was performed for Sema3A using normal skin and skin cancer specimens.
Results: In NHEK, *SEMA3A* expression was elevated by high calcium concentration and reduced by low calcium condition, while *NGF* expression was not dependent on calcium. Their expressions were unchanged by calcium in NHFb. Immunohistochemically, keratinocytes in the prickle layer of normal epidermis and squamous cell carcinoma cells were positive for Sema3A, sparing basal cells and suprabasal cells. The addition of histamine to NHEK at 10 μg/ml enhanced *SEMA3A* expression but depressed *NGF* expression. In NHFb, however, histamine decreased both *NGF* and *SEMA3A* levels.
Conclusions: Sema3A inhibits C-fiber elongation/sprouting in the upper layers of the epidermis, where calcium concentration is high, thereby determining the nerve endings. Histamine reduces Sema3A production by fibroblasts, allowing C-fibers to elongate in the dermis. In contrast, the histamine-augmented keratinocyte production of Sema3A might suppress C-fiber elongation and exaggerated pruritus.

1. Introduction

C-fiber is known as a primary afferent nerve to deliver itch to the central nerve system [1]. Numerical increment and elevated sprouting of C-fiber in the epidermis easily produce itch and accelerate the itch–scratch cycle [2]. In addition, C-fiber plays pluripotential roles for itch-related events. For example, neuropeptides released from C-fibers stimulate keratinocytes and mast cells to produce pruritogenic factors that again stimulate C-fiber [3–5].

Both neurotrophins and chemorepellents regulate the elongation and sprouting of itch-associated C-fibers in the skin. Nerve growth factor (NGF) [6,7] and semaphorin 3A (Sema3A) [8] are representatives of these two types of nerve axon-guidance factors, respectively. NGF and Sema3A have opposite effects on C-fiber elongation, which is related to promotion of itch in the skin. In atopic dermatitis, the number of peripheral nerve endings is increased and may amplify itch [2]. NGF is known to initiate the sprouting of epidermal nerve fibers in atopic dermatitis and its model NC/Nga mice [9]. Changes in Sema3A expression/production has also been reported in the lesional skin of atopic dermatitis [10,11]. A reduction in Sema3A expression allows nerve fibers to sprout into the upper epidermis, and photochemotherapy may exert a therapeutic effect by increasing epidermal cell production of Sema3A [12]. On the other hands, in normal skin, the extracellular calcium concentration critically determines a variety of biological activities of keratinocytes [13]. The calcium concentration increases towards the outer epidermis, forming a "calcium gradient" within the epidermis [14]. It is possible that this physiological condition influences on the production of the nerve guidance factors. In addition, histamine released from mast cells in certain allergic conditions possibly modulates their production.

To address the regulatory mechanisms underlying C-fiber elongation, we investigated the effects of calcium concentration on the expression of *NGF* and *SEMA3A* in normal human epidermal keratinocytes (NHEK). Upon allergic stimulation, histamine and

* Corresponding author. Tel.: +81 93 691 7445; fax: +81 93 691 0907.
E-mail addresses: tokura@med.uoeh-u.ac.jp, jsid@mbox.med.uoeh-u.ac.jp (Y. Tokura).

0923-1811/$36.00
doi:10.1016/j.jdermsci.2010.11.012

tryptase are produced by mast cells, and keratinocytes express H1 receptors for histamine and protease-activated receptor-2 (PAR-2) for tryptase [15,16]. Therefore, it is an interesting issue to investigate the effects of histamine and a PAR-2 agonist, SLIGRL-NH_2 (SLIGRL) on the expression of these guidance factors in NHEK and normal human fibroblasts (NHFb). Results suggest that the physiological and pathological conditions of the skin modulate the production of NGF and Sema3A by keratinocytes and fibroblasts.

2. Material and methods

2.1. Chemicals

Histamine and a PAR-2 agonist SLIGRL were purchased from Wako (Osaka, Japan) and Tocris (Ellisville, MO), respectively. These substances were freshly diluted by distilled water before use.

2.2. Cell and cell culture

Primary culture of NHEK was obtained from Lonza (Basel, Switzerland). NHEK were grown in Keratinocyte Growth Medium-2 (KGM-2) for expansion and Keratinocyte Basal Medium-2 (KBM-2; Lonza) for experiments at 37 °C in a 5% CO_2 atmosphere. Primary NHFb were obtained from Takara (Osaka, Japan) and cultured in Dulbecco's Minimum Essential Medium (DMEM) supplemented with 10% fetal bovine serum, 100 U/ml penicillin, 100 μg/ml streptomycin and 2 mM glutamine.

2.3. Real-time quantitative reverse transcription-polymerase chain reaction (RT-PCR) analysis

NHEK were grown to subconfluence in KGM-2, unstimulated or stimulated with histamine or SLIGRL under various calcium concentration in KBM-2, and then harvested. cDNA was synthesized directly from cell lysate solution using TaqMan Gene Expression Cells-to-CTTM Kit (Austin, TX) according to manufacturer's instructions. The conditions of reverse transcription were as follows: 60 min at 37 °C, 5 min at 95 °C, and then hold at 4 °C. Amplification reaction was performed using ABI PRISM 7000 Sequence Detection System (Applied Biosystems; Carlsbad, CA) with TaqMan Gene Expression Assays (Applied Biosystems). Primers and TaqMan probe for human *SEMA3A* and human *NGF* were purchased from Applied Biosystems. Amplification of human β-actin, *ACTB* (TaqMan β-actin Control-Reagent Kit) was used as an endogenous control for quantification. The conditions of the real-time PCR were as follows: 2.0 min at 50 °C (reverse transcription), 10 min at 95 °C (RT inactivation and initial activation), and then 40 cycles of amplification consisting of 15 s at 95 °C (denaturation) and 1 min at 60 °C (annealing and extension). All heating and cooling steps were performed with a slope of 20 °C/s. Samples were analyzed in triplicates and averages were calculated for analysis of the expression ratios.

2.4. Western blotting

NHEK were cultured at 0.15 mM or 0.6 mM of calcium concentration in 6-well plates for 12 h, harvested with rubber policeman, and subjected to extraction by RIPA buffer (50 mM Tris–HCl [pH8.0], 150 mM sodium chloride, 0.5 w/v% sodium deoxycholate, 0.1 w/v% sodium dodecyl sulfate, and 1.0 w/v% NP-40 substitute; Wako Chemical Co., Tokyo, Japan). Ten μg protein samples were electrophoresed by 8% SDS-polyacrylamide gel electrophoresis and electroblotted onto polyvinylidene difluoride membranes for 2 h at 180 mA. After blocking with 5% skim milk solution, the membranes were incubated with rabbit anti-human Sema3A (sc-28867; 1:1000, Santa Cruz Co., Santa Cruz, CA), NGF (sc-548; 1:1000), or Loricrin (PRB-145P; 1:1000, Covance, NJ) polyclonal antibodies, and the reaction was detected with horseradish peroxidase-conjugated goat anti-rabbit IgG (1:3000, Bio-Rad, Hercules, CA). Immunoblots were visualized using the ECL Plus Western Blotting Detection Reagents (GE Healthcare, Buckinghamshire, England) according to the manufacturer's protocol.

2.5. Cytometric beads array

IL-8 and GM-CSF concentration in the culture supernatants were determined with Cytometric Bead Array (CBA) Flex Set System purchased from Becton Dickinson and Company (Franklin Lakes, NJ) using FACSCanto (Becton Dickinson).

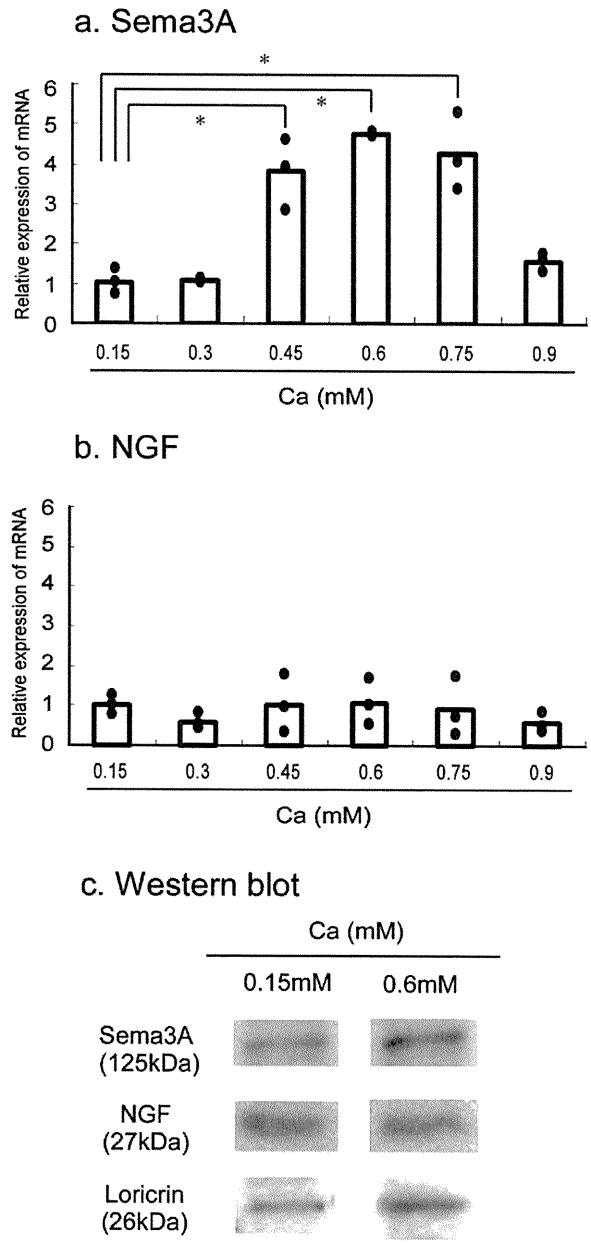

Fig. 1. Effects of calcium concentration on the expression of *SEMA3A* and *NGF* in NHEK. NHEK were cultured under varying concentrations, ranging from 0.15 to 0.9 mM for 2 h. After harvesting, cDNA was synthesized directly and the expression of *SEMA3A* (a) and *NGF* (b) was assessed by real-time PCR. The data are expressed as (expression level of 0.3–0.9 mM calcium group)/(expression level of 0.15 mM calcium group). Bars represent the means of three independent experiments. $^*P < 0.05$. The expression levels of Sema3A, NGF, and loricrin in NHEK cultured under 0.15 or 0.6 mM calcium were analyzed by Western blotting (c).